JAAS

Accepted Manuscript

This is an *Accepted Manuscript*, which has been through the Royal Society of Chemistry peer review process and has been accepted for publication.

Accepted Manuscripts are published online shortly after acceptance, before technical editing, formatting and proof reading. Using this free service, authors can make their results available to the community, in citable form, before we publish the edited article. We will replace this *Accepted Manuscript* with the edited and formatted *Advance Article* as soon as it is available.

You can find more information about *Accepted Manuscripts* in the Information for Authors.

Please note that technical editing may introduce minor changes to the text and/or graphics, which may alter content. The journal's standard Terms & Conditions and the Ethical guidelines still apply. In no event shall the Royal Society of Chemistry be held responsible for any errors or omissions in this *Accepted Manuscript* or any consequences arising from the use of any information it contains.

ROYAL SOCIETY OF CHEMISTRY

www.rsc.org/jaas

Basic mechanisms of signal enhancement in ns double-pulse laser-induced breakdown spectroscopy in gas environment

Elisabetta Tognoni*, Gabriele Cristoforetti

National Institute of Optics of the National Research Council (INO-CNR)

Via G. Moruzzi 1, 56124 Pisa, Italy

**corresponding author; e-mail: elisabetta.tognoni@ino.it*

Tel +39 050 3152223, Fax +39 050 315 2576

Abstract

Understanding the mechanisms of the signal enhancement in double-pulse laser-induced breakdown spectroscopy (DP-LIBS) is highly desirable. It is evident, however, that it is not possible to fit a unique general model to the observations obtained in collinear or in orthogonal geometries, in pre-spark or in re-heating scheme, using ns or fs pulses, in gas or in liquid environment. We believe, instead, that by considering separately the specific experimental cases (for example: a given irradiation geometry, a given pulse timing, etc.) the comprehension of the processes occurring during double-pulse experiments might become easier. We focus on one specific experimental case, namely ns double-pulse irradiation of solid targets in gaseous environment, and classify the experiments according to the irradiation mode (orthogonal pre-spark, collinear and orthogonal re-heating). Then, we propose a description of the processes occurring in the different cases, on the basis of data and interpretations that are available in the literature.

1. Introduction

Double-pulse (DP) irradiation in the analytical exploitation of laser-induced plasmas was firstly proposed in 1969 by Piepmeier and Malmstadt. The intensity of the emitted spectral lines was found to increase when focusing on a solid target in air nanosecond double or multiple laser pulses mutually delayed by hundreds of nanoseconds up to several microseconds [1]. Many studies in the wider field of laser ablation have followed this pioneering work. The use of DP irradiation to improve the performance of techniques like laser ablation inductively coupled plasma (LA-ICP), laser micromachining or pulsed laser deposition (PLD) is described elsewhere [2-5]. In the present paper we focus on the use of DP in Laser-Induced Breakdown Spectroscopy (LIBS). During recent years a great effort has been devoted to elucidate the mechanisms that yield the signal enhancement in DP-LIBS [6-10]. Of course, understanding the basic mechanisms would allow one controlling the analytical performance and maximising the advantages of double-pulse irradiation. Extensive reviews of the available literature have been compiled [11-14], aiming at a synthesis of the different observations. It is evident, however, that it is not possible to fit a unique general model to the observations obtained in collinear or in orthogonal geometries, in pre-spark or in re-heating scheme, using ns or fs pulses, in gas or in liquid environment. We believe, instead, that by considering separately the specific cases (for example: a given irradiation geometry, a given pulse timing, etc.) the comprehension of the processes occurring during double-pulse experiments might become easier.

Therefore, in this review we limited our scope to one specific experimental case, namely ns double-pulse experiments on solid targets in gaseous environment. The readers interested in other experimental cases are referred to the relevant literature. For example, the mechanisms involved in fs and ps double-pulse experiments have been discussed in some detail in ref. [11]. The advantages offered by double-pulse for the analysis of metallic targets submerged in water have been well described in refs.[13,15]. The effect of double-pulse in pure gas and in presence of aerosols has

been investigated in [16], while the characteristics of a double-pulse plasma produced by irradiation of a solid target in vacuum have been studied in ref. [17].

Though the case of ns double-pulse measurements in gaseous environment was already included in the reviews published some years ago by Babushok et al. and by Scaffidi et al. [11,12], we here propose a different approach. We are not going to introduce a new interpretation of the double-pulse signal enhancement, because the main processes occurring during ns DP-LIBS have already been identified and described in the literature since several years (see for example refs.[18-24]). Rather, we classify the DP-LIBS experimental configurations according to the irradiation mode (orthogonal pre-spark, collinear and orthogonal re-heating) and then propose a description of the processes occurring in the different cases, on the basis of data and interpretations that are available in the literature. Even so, in each configuration several different processes must be considered.

In the first part of the review we shortly recall the processes that are involved in the formation of a laser-induced plasma, which of course also take part in the double-pulse phenomenology. During the initial instants of the laser pulse, photon energy is delivered to the target; during the trailing part, instead, the absorption of photons typically occurs in the plume formed in front of the target. According to the literature, the switch between the two regimes depends not only on the interaction between the laser pulse and the sample, but also on the buffer gas surrounding the sample [25-28]. Section 2 recalls some fundamental points regarding the laser shielding produced by the plasma in front of the sample, which affects the ablation efficiency and the plasma temperature. After the end of the laser pulse, when the energy supply to the plume is finished, the evolution of the system is well described by the expansion of the plume, which drives also a shock wave in the surrounding environment, as recalled in section 3. The expanding shock wave produces a modification of the buffer gas conditions, with direct consequences on the characteristics of the interaction between the second pulse and the target. In addition, since thermal effects on the target surface have also been indicated to contribute to the double-pulse phenomenology, in section 4 we overview recent findings on the dependence of LIBS spectra on sample temperature.

On the basis of this preliminary discussion, the specific double-pulse plasma issues are addressed. Section 5 is dedicated to the topic of signal enhancement under DP irradiation. It is not a list of enhancement records, but rather a discussion of some relevant issues, which are intended to facilitate the comprehension of the following. Section 6 begins with the description of the pre-spark orthogonal geometry, which is probably the easiest one to understand because the two pulses are well distinguished in the effects they produce. Then, we take into consideration the case of collinear pulses. Even though this is a more complicated case, many characteristics can be satisfactorily explained by taking into account the same processes that are proposed to describe the pre-spark orthogonal case. The case of DP re-heating in orthogonal geometry is then depicted. In describing the main characteristics found with different configurations, we preferred to keep the text as plain as possible, sketching the essential elements of the "ideal" case. In the sub-sections following the description of each geometry, several relevant references have been mentioned, according to a chronological order, in order to provide a guide to specific issues. In any case, a complete overview of the literature regarding nanosecond DP-LIBS is out of the scope of the present work. We point the interested reader to the above mentioned reviews [11-12].

2. The laser shielding during the ablation of a solid target

During laser ablation, target heating, vaporization and plume expansion take place simultaneously, making an accurate description of the process very difficult [29]. In the following, however, we assume that laser light absorption by the target, vaporization and plasma formation proceed much faster than the expansion of the ablated material. Under this approximation, the two stages of plasma formation and expansion of the ablated particles in the background gas can be decoupled for an easier description [30]. The plasma formation and the resulting laser shielding (which occur for times shorter than the pulse width, $t \leq \tau_{pulse}$) are the object of the present section, while the shock wave formation and the plume expansion (occurring for $t > \tau_{pulse}$) are the topic of section 3.

2.1 Laser shielding mechanisms

Let's consider the irradiation of a solid target with a ns pulse. The time scale for electronic absorption of laser photons is of the order of a few fs and the time scale for lattice thermalization is of the order of a few ps [29, 31, 32]. Thus, during the pulse, the conduction and valence electrons inside the sample gain energy by absorbing photons and transfer it to the surrounding lattice, thereby heating the irradiated volume and leading to target vaporization. At low laser irradiance this description is valid for the whole pulse duration; however, for increasing irradiance, a threshold is encountered corresponding to the plasma ignition (this occurred at $0.3 \cdot 10^8$ W cm^{-2} in the measurement shown in ref. [33]). From the time of ignition up to the end of the pulse, a portion of the laser energy is absorbed by the plasma, so that the target surface is partially shielded ("plasma shielding"). The two dominant photon absorption mechanisms in laser-produced plasmas are photoionization (PI) and inverse bremsstrahlung (IB). Photoionization involves the absorption of a photon by an excited particle with the release of an electron. The IB process, instead, involves the absorption of photons by free electrons, during collisions with neutral or ionized atoms. Appropriate formulas describing the above mentioned mechanisms have been elaborated by several authors [30,34-40]. Here, we report a simplified version, with the purpose of outlining the dependence of absorption coefficients on the main plasma parameters. In this view, the absorption coefficients for photoionization, electron-ion IB and electron-neutral IB can be expressed, respectively, as [41]:

$$\alpha_{PI} = C\sum_{Z=1}^{2}\frac{\lambda^3 Z^2 n_e n_Z}{\sqrt{T}}\overline{G_{fb}}\left[e^{\frac{hc}{\lambda k_B T}} - 1\right] \quad (1)$$

$$\alpha_{IB,e-i} = C\sum_{Z=1}^{2}\frac{\lambda^3 Z^2 n_e n_Z}{\sqrt{T}}\overline{G_{ff,e-i}} \quad (2)$$

$$\alpha_{IB,e-n} = CA\frac{\lambda^3 n_e n_0}{\sqrt{T}}\overline{G_{ff,e-n}} \quad (3)$$

where n_e, n_Z and n_0 are the electron, ionic (with charge Z) and neutral atoms number density, λ is the laser wavelength, T the plasma temperature, h and k_B are Planck's and Boltzmann's constant, c the

speed of light, C is a constant and $\overline{G_{fb}}$, $\overline{G_{ff,e-i}}$, $\overline{G_{ff,e-n}}$ the free-bound and the free-free Gaunt factor in the cases of electron-ion and electron-neutral interaction, respectively. For further details the reader is pointed to ref. [41]. It is not easy to give an estimate of the actual values of these coefficients, because many of the parameters vary in space - in the plume volume - and in time - during the laser pulse. This large variability is also reflected in the results reported in the literature. According to some authors, in typical LIBS plasma conditions the IB coefficient for electron-neutral interaction is much smaller than that for electron–ion interaction (except at the very beginning of the target evaporation) and can be neglected [30,36,37]. The numerical simulations carried out by Bogaerts and co-workers show, instead, that electron-neutral IB is the dominant absorption process especially for the 266 nm wavelength and at a low laser irradiance [34,35]. It is evident that the specific experimental conditions (or the parameters used in a simulation) determine the relative strength of electron-neutral IB and electron-ion IB. However, the dependence of the IB absorption coefficients on λ^3 suggests that this mechanism is much more efficient for infrared laser wavelengths. Due to the exponential dependence on the laser frequency, photoionization is often considered as the dominant absorption mechanism for UV radiation [30].

The contribution of Mie absorption, which is given by small condensed clusters inside the plasma, has been also suggested to explain the behaviour observed with UV laser wavelength, especially at low plasma temperature [39, 40 and references therein] and at the beginning of the laser pulse [37].

2.2 Laser Supported Detonation

For irradiances just above the plasma ignition threshold, plasma absorption is already present but it affects only a small fraction of the pulse energy, as suggested by the observation that in this range the depth of the crater increases with laser irradiance [33]. However, the absorption mechanisms mentioned in section 2.1 depend on the density of the particles in the plasma. When the laser irradiance is high enough that the dense plasma created by the initial part of the pulse absorbs a

substantial fraction of the laser photons during the remaining part of the pulse, a second change of regime is observed. The threshold for this change of regime has been measured by different groups and for different wavelengths, resulting in values ranging between 0.3 GW cm^{-2} [29] and 0.8 GW cm^{-2} [27,33,42] for ablation at atmospheric pressure. The energy accumulated in the plasma by means of photon absorption leads to the expansion of the ablated matter in the buffer gas environment, giving origin to the formation of a shock wave (see section 3). The passage of the shock wave results in the heating of the buffer gas atoms and in the production of a small number of free electrons. In this way, the gas layer immediately behind the shock wave becomes able to absorb laser photons, being excited and ionized as well, giving rise to a new plasma shell, which in turn pushes the shock wave front and feeds the avalanche process [43]. This regime is called Laser-Supported Detonation (LSD). When this occurs, most of the laser pulse energy is absorbed in the plasma layer facing the focusing lens, so that the plasma mainly grows in the direction of the incoming laser pulse, with the result that a great number of air atoms/ions are engulfed into the plasma. A further difficulty in the modelling of the phenomenon is that in typical LIBS conditions the time needed for initiation of the laser-supported detonation regime is comparable with the ns pulse duration [44-46].

According to an alternative model, the photon absorption is only caused by the matter ablated from the target, which therefore expands in the surrounding gas like a piston, simply pushing out the gas atoms or molecules. This description is generally preferred by modelists [47], because quantifying the interplay between ablated vapour and ambient gas, especially at atmospheric pressure, is a very challenging task. Experiments devoted to the spatially resolved characterization of the plasma have been carried out to check whether buffer gas and target atoms are mixed in the plasma plume or confined in separate shells. In some cases the spatial distributions of target and buffer gas species were found to substantially overlap in the plasma [27, 48, in air], while in other cases they were separated [49, in argon]. It is likely that different models are appropriate in different experimental conditions: recently Yu and co-workers observed that LSD regime was settled during laser ablation

of an Al target with the fundamental Nd:YAG wavelength, while atoms ablated from the target and buffer gas atoms were spatially segregated when using the Nd:YAG third harmonic at a similar irradiance value [41].

In LSD regime, the pulse energy impinging on the target decreases by the amount absorbed in the plume and the ablation is strongly reduced [50]. The morphology of the craters was also found to change when the irradiance overcome the threshold for the ignition of LSD, suggesting that a change in the mechanism of mass removal from the target occurs [33]. Below the threshold, melt effects on the surface are negligible and phase explosion seems to be the only mechanism able to justify the observed ablation rate (2–4 μm depth per pulse). Above the threshold, instead, melt displacement and expulsion progressively become dominant, as indicated by the crater rims formed by re-solidified material and by melt droplets splashed on the target around the crater. The strong decrease of the ablation rate suggests that in this range phase explosion becomes less efficient. This change can be explained by considering that under LSD conditions melt splashing is favoured by the formation of a hot high-pressure plasma, while the reduced effective irradiance on the target is not sufficient to ignite phase explosion. By increasing further the irradiance by about one order of magnitude, the line intensity and the atomized ablated mass are found to increase again. This behaviour can be explained as the effect of a saturation of the photon absorption by the plasma, which causes a second increase of the effective irradiance reaching the target surface, with a new regime of phase explosion [33]. However, it has been suggested that multiple ablation mechanisms might co-exist, especially under high irradiance conditions and especially when using laser pulses with non flat energy distribution (like in the Gaussian case) [51]. The ejection of material from the centre of the irradiated area might also be temporally separated from ejection occurring along the periphery of the laser spot.

Finally, it is worth noting that the absorption coefficients in eqns. (1-3) show the dependence of plasma shielding on the laser wavelength. Many experimental works (see for example refs.[36, 52, 53]) reported a lower ablation depth for IR laser plasmas than for UV plasmas produced at similar

laser intensity. These observations suggest that, overall, the absorption mechanisms are more efficient for infrared than for visible and UV lasers.

2.3 The laser shielding in dependence on gas density

The number density of the ambient gas affects the LSD threshold: as said above, in presence of a low particle density the absorption of the photons is less effective, resulting in a higher irradiance threshold for LSD ignition. This is indirectly illustrated by the trend of atomized matter versus fluence for different values of the ambient pressure, plotted in Figure 1. The threshold irradiance values can be estimated in correspondence of the fluence at which the atomized mass abruptly falls, by considering a pulse width of 50 ns. The measurement was carried out at a constant ambient temperature of 20 °C, so that for the datasets obtained in single pulse mode (labelled SP in the figure) the pressure values are directly proportional to the values of gas number density. This doesn't apply to the DP case, where the second pulse is delivered in the environment modified by the first pulse. For SP ablation carried out at atmospheric pressure (solid squares), the threshold for the onset of strong shielding can be recognized at a fluence of about 50 J cm^{-2} (irradiance of about 1 GW cm^{-2}), where the ablated mass drops off. At high fluence (> 500 J cm^{-2}) the ablated mass increases again as an effect of saturation of the plasma absorption [33]. For an air pressure value of 500 torr (empty squares), the shielding threshold is slightly shifted at about 60 J cm^{-2}. For pressure values lower than 300 torr no change of regime can be found in the range of fluence investigated: the atomized matter in the plume displays instead a monotone increasing trend with laser fluence. This suggests that no LSD regime is established, for the experimental conditions in ref. [54], at ambient pressure lower than 300 torr. Looking at the dataset obtained under DP irradiation (empty stars in Fig.1), we note a close similitude with the behaviour obtained under SP irradiation at 100 torr. The reason of this similarity is discussed in section 3, in relation to the rarefied volume located at the centre of the expanding plasma.

According to Bindhu et al. [55], different absorption mechanisms become dominant at different pressure of the ambient gas: the cascade-like process at high pressures, multiphoton ionization at lower pressures.

Beside number density, the laser shielding depends also on the type of buffer gas. Iida found out that the amount of mass ablated from an aluminium alloy was much larger in helium atmosphere than in air or argon at the same pressure and temperature and fixed laser fluence [25]. Gravel and Boudreau confirmed this finding by observing that LSD was ignited at a much lower irradiance in air and argon than in helium gas [50].

2.4 The laser shielding in dependence on target material

The extent of the shielding effect depends not only on the experimental variables (buffer gas composition and pressure, laser wavelength and irradiance) but also on the sample nature [56]. Iida investigated the ablation behaviour of several materials, including metals and ceramics, in presence of different Ar pressure values [25]. For the metal samples, the ablated mass was strongly affected by the ambient pressure, but for the ceramic samples such an effect was relatively small. According to the author, this finding reflects the influence that the sample characteristics have on the beginning of plasma generation process, i.e. on the creation of the initial electrons that determine a cascade-like growth of the electron number density. The laser absorption in the ceramics is a volumetric process, while for metals it occurs in a surface layer. Then, the power density of laser radiation at target surface is higher for metals and breakdown occurs more easily for metals than for ceramics. In turn, the electron number density grows more rapidly for metals, and the shielding becomes more important. Therefore, the ablation of metallic samples is strongly favoured by a reduction of the gas pressure, while for ceramics the effect is much lower.

Among metals, different behaviours are expected as a function of their thermal diffusivity. This property determines the speed of heat diffusion from the target surface to the bulk and, in turn, the spatial distribution of the temperature inside the target and the depth of the molten metal pool.

Under laser irradiation at a fixed fluence, a metal target with a low thermal diffusivity (such as Mn, Fe or Co) tends to have a higher surface temperature and a thinner molten pool with respect to metals characterized by higher values of such parameter (such as Cu, Al or Au). Therefore, at atmospheric pressure, metals with low thermal diffusivity are expected to reach more easily the conditions for the occurrence of phase explosion and thus give larger values of ablated mass than metals with high thermal diffusivity [57]. By investigating the characteristics of the plasmas produced on Al, Cu and Ni under the same experimental settings, Aguilera et al. observed an inverse proportionality between the temperature reached by the plasma and the ablation rate. For example, the most important plasma shielding occurred for the Cu matrix, so that the number of target atoms in the Cu plasma was the lowest of the three matrices and the temperature was the highest one [58].

3. The characteristics of an expanding plasma

In this section we recall some basic points regarding the expansion law of the laser-induced plasma in the surrounding gas. In particular we look at the time following the end of the pulse and assume that the pulse energy has been released in a short time and in a small volume compared to the time and space scales of the plasma expansion.

At the end of the laser pulse the energetic high pressure plasma expands compressing the surrounding gas atoms and leading to the formation of a shock wave (SW). In the early stage (a few tens ns from the laser pulse) the shock wave expands with almost constant velocity, irrespective of the background gas pressure [59]. During the expansion, energy is progressively dissipated by doing work against the ambient gas and by heating/ionizing it [60]. At the beginning, the shock wave and the internal plasma expand together; later, the SW detaches from the plasma and continues to expand, while the plume expansion stops at a radius of the order of 1 mm, depending on the experimental conditions [61]. Then, as far as the expansion reduces the pressure of the region behind the SW front, the shock wave velocity slows down until it becomes a sonic wave [47]. The

evolution of this phenomenon can be well described by the point strong explosion theory, formulated by Sedov [62,63]. According to this theory, the position R of the expanding shock wave at a given time t is:

$$R = \xi_0 \left(E_0/\rho_0\right)^{\frac{1}{2+\zeta}} t^{\frac{2}{2+\zeta}} \qquad 4$$

where ξ_0 is a constant which depends on γ, the specific heat ratio of the background gas, E_0 is the energy deposited in the wave and ρ_0 is the density of the unperturbed background gas. The parameter ζ depends on the geometry of the shock wave expansion: $\zeta = 3$ for a spherical shock wave expansion, $\zeta = 2$ for a cylindrical expansion and $\zeta = 1$ for the planar expansion case. Therefore, the radius for a spherical shock wave is proportional to $t^{0.4}$. When irradiating a solid target, in the first stage of the shock wave expansion (until about 100 ns from the laser pulse) the geometry can be assumed to be planar; later the spherical geometry is a better approximation [64]. Since in double-pulse, in the great majority of cases, the inter-pulse delays are longer than 100 ns, in this framework we are mainly interested in the stage of expansion with spherical symmetry and in the following we therefore describe only this one.

The Sedov model has been often used to describe the expansion law of a shock wave propagating in a homogeneous environment [23,65,66]. For the sake of example, the shadowgraphic image reported in Fig. 2 shows the expansion of both the plume and the shock wave produced by focusing a ns laser pulse in air a few mm above a planar surface (the surface edge is on the right side of each frame). The plume is roughly coincident with the bright spot (due to bremsstrahlung emission), while the shock front is visible as a bright circle. The values of the radii of plume and SW at different times have been estimated from the frames of Fig. 2 and shown in Fig. 3. The experimental values of the SW radius are in good agreement with the expansion law predicted by eqn. (4): the best fitting of the data with a curve of the type $R = at^b$, indicated in Fig. 3 by a dashed line, gives for the exponent b the result 0.4 ± 0.02 [66]. The plume evolution is qualitatively in agreement with a drag model, as observed also by other authors [61].

The profiles of pressure, temperature and gas density predicted by the Sedov model at the shock front and in the region behind it, have been found to correctly describe both the experimental observations and the results obtained by numerical simulation of an expanding laser-induced plasma [61]. Figure 4 displays a qualitative picture of the model predictions for the initial phase of expansion, where the volume enclosed in the shock wave is divided in two concentric regions and the internal one (region 2) coincides with the plasma plume. Going from region 1 to region 2, a steep increase of temperature is encountered at the plume boundary; the pressure, instead, shows its steepest gradient just behind the front and its value inside the plume is higher than in the unperturbed gas (region 0 in Fig.4). Since pressure, temperature and density are related through the ideal gas law, a decrease of gas density in the core is also predicted. Thus, the shock wave front is characterized by a large gas density, but inside the plume the density steeply drops off to values much lower than the unperturbed medium. This picture is representative of the early expansion stages; later on, the particle number density starts growing in region 1 and then also in region 2, until its profile becomes flat on the level of the unperturbed medium (see ref. [62], page 272). Under the assumption that either the gas in the unperturbed environment and the plasma plume can be described as ideal gases, the rarefaction in the core of the plume can be estimated by combining the Sedov theory and the ideal gas law. We also assume that the region of the plume is homogeneous in pressure, temperature and density. According to the strong explosion theory, the pressure of the *SW* front (P_{SW}) and the pressure of the unperturbed environment $P_{\substack{unperturbed\\environment}}$ at a given instant of the evolution are linked by the relation:

$$P_{SW} = \frac{(2\gamma M^2 - \gamma + 1)P_{\substack{unperturbed\\environment}}}{\gamma + 1} \qquad 5$$

where γ has been already defined and M is the SW Mach number (dependent on time) that can be calculated by fitting the growth of the shock wave radius in time. The Sedov theory also predicts that in the initial phase of expansion, the pressure value in the internal region (region 2 in Fig. 4)

can be approximated as a fraction of the pressure of the *SW* front: $P_{plume} \approx 0.365\, P_{SW}$. Therefore, we have a means to calculate the P_{plume} from the observed SW expansion law. In addition, if the temperature of the plasma is also known, the relation based on the ideal gas law:

$$\frac{n_{plume}}{n_{\substack{unperturbed \\ environment}}} = \frac{P_{plume}}{P_{\substack{unperturbed \\ environment}}} \frac{T_{\substack{unperturbed \\ environment}}}{T_{plume}} \qquad 6$$

allows us determining the particle number density in the plume, n_{plume}.

Values of the ratio $n_{plume} \Big/ n_{\substack{unperturbed \\ environment}}$ calculated for typical experimental conditions (measurements in air, at a delay of a few μs after the laser pulse) range from 0.04 to 0.07. Such values reveal that the gas number density inside the laser plasma in typical LIBS conditions is similar to the density of gas at room temperature at about 50 torr pressure [67].

As displayed in Fig.4, particle number density and pressure show different profiles. The temperature inside the shock wave volume, in fact, is higher than that of the unperturbed gas; as a consequence, even though the pressure behind the shock front is higher than outside (this is the mechanism that drives the outward expansion of the shock wave), the particles number density in the plume is much lower than in the unperturbed environment gas. This is an important point in view of the occurrence of laser-shielding, which, as discussed in section 2, depends on the particle density.

When focusing a laser pulse in a gas (as in the case of the pre-spark in orthogonal DP configuration) a spherical shock wave expansion is a good model. However, when the laser pulse is focused in the neighbourhood of a solid surface, the reflection of the propagating shock wave must be taken into account. In Fig. 2, the interaction of the shock wave with the surface is clearly visible from frame 3 on. When the expanding shock wave reaches the target, the mass contained at the shock front starts to pile-up at the target surface until a reflected wave which moves backward is formed. Numerical models [68,69] of shock wave reflection reveal that such an initial accumulation of mass at the target surface forms a gas layer characterized by pressure and density higher than the original shock

front. Experimentally, this is confirmed by the presence of a bright layer near the target (indicating high density in Schlieren shadowgraphic imaging) in frames 3 and 4 of Fig. 2, while the regular reflected wave is evident in frames 5 and 6. At the time of frame 5, the density at the contact layer starts to decrease until a rarefaction is produced when the reflected wave detaches from the surface. Frames 7 and 8 also show the presence of the non-regular reflected wave, known as Mach wave [70]. The time needed for the shock front to reach the target surface depends of course on the energy of the wave, on the density of the ambient gas and on the distance between the laser focal spot and the target.

4. The effects of the target surface temperature

It has been observed that heating metallic or glass samples up to temperatures in the range 300-1400 °C leads to a significant increase in spectral line intensity [71-77], in signal to noise ratio [78], in plasma temperature [72], in plume size [75] and in ablation rate [71, 74,76]. In fact, less energy is needed to bring the sample temperature closer to the melting point. In addition, the reflectivity for some metals tends to decrease with rising temperature [75], so that the coupling of the laser energy with the target is improved.

Sanginés et al. also observed that, for a fixed pulse energy, the plasma electron density decreases with increasing the temperature of an aluminium sample [78]. The authors explained this finding as a result of a faster plasma expansion. In fact, since the target is inside a furnace, the air in front of it is heated as well; therefore, assuming an ideal gas behaviour, the speed of the plasma's shock wave front increases up to a factor of about 1.6 at 500 °C due to the reduced gas density (see eqn. (4)). For the same reason, the stop distance of the shock wave expansion increases as well, so that the final plume size also increases, as observed by Eschlböck-Fuchs et al. for heated samples [75]. However, we didn't find in the literature any mention of another mechanism that might contribute to the behaviours observed at increasing sample temperature: the reduction of laser shielding. In fact, if, according to the ideal gas law, the gas density in front of a heated sample is locally reduced

compared to the room temperature value, then the laser shielding is also reduced, similarly to what is found in experiments at reduced pressure [79]. To give a quantitative example, we recall that at a temperature of 1000 °C the gas density is reduced by a factor of about 4 with respect to the room temperature condition. On the one hand, the effect of the reduced laser shielding might explain the observed decrease in electron density. On the other hand, it may sum with the direct effect of the temperature on the target surface softening, in favour of an increase of the ablation volume.

Krstulovic and Milosevic investigated the dependence of the drilling process on the laser repetition rate in the range between 1 and 20 Hz with a titanium sample in vacuum [80]. For a given value of the total number of pulses delivered to the target, the largest ablated volume was observed for the highest repetition rate, i.e. the lowest pulse-to-pulse interval, despite the fact that the effective laser pulse energy measured at 20 Hz was 10% lower than at 1 Hz. The authors suggested that the ablation threshold was decreasing during the continuous irradiation, because of the progressive heating of the target surface (in agreement with the results obtained by Brygo et al. [81]). Since the experiment was carried out in vacuum, thermal effects acting on the target surface were the only explanation of the observed variation in ablation efficiency [80].

This interpretation is in agreement also with the results obtained by Klimentov et al., who investigated the dependence of the ablation depth per pulse on the laser repetition rate, in a range spanning from 5 to 2000 Hz, for a steel sample, at different pressure values. The greatest effect on the ablation depth per pulse was here produced by the ambient gas pressure; however, the increased ablation rate observed in vacuum for increasing repetition rate revealed that the increase of the target surface temperature also produced a measurable effect on the ablation efficiency [82].

In summary, when considering collinear DP irradiation, thermal effects produced by the first pulse on the sample surface cannot be disregarded, though they are very hard to quantify.

5. Measurement of the analytical performance

In the abundant literature regarding DP-LIBS, many works investigate the physical processes and much more deal with the analytical performance of the technique. Though this paper belongs to the first group, the analytical investigations are extremely important to validate the theoretical description that we propose for the different DP configurations. Therefore, it is worth to spend a few words about some analytical issues.

Double-pulse LIBS has been introduced in laboratory practice to improve those figures of merit that, in single pulse LIBS, are deemed not satisfactory for qualitative or quantitative analysis. These include limits of detection (LODs) and signal reproducibility [83-85]. By inspection of the relevant literature, however, only in rare cases the enhancement or suppression of the noise is reported, as a complementary information with respect to line enhancement [20, 86, 87]. Similarly, infrequent is the comparison of the reproducibility obtained in SP and DP configuration; according to refs. [20, 88-90], reproducibility seems to be improved in DP case.

There is a general consensus on the improvement of LODs that can be achieved by using DP-LIBS. Papers reporting this kind of achievement are useful to the whole scientific community (a relevant list can be found in ref. [12]). In some cases, however, researchers have quantified the DP enhancement of a resonance line of the matrix element. It may even happen that, when the signal enhancement is lower than expected, the presence of unidentified mechanisms is invoked to explain the experimental findings. However, there are two main phenomena that should be considered before searching for more exoteric interpretations: self-absorption and ionic species population balance. The issue of self-absorption was scarcely considered in the earlier works regarding double-pulse enhancement. However, the sensibility of the experimentalists toward this issue gradually changed [91]. For example in ref. [92] the Mg line intensity dependence on the inter-pulse delay was studied on a sample where the Mg concentration was 19 ppm, so to rule out any concern about self-absorption effects; in ref. [84], Gautier et al. reported a strong dependence of the degree of self-absorption of a resonant Si line on the inter-pulse delay. The self-absorption degree may increase or

decrease under DP irradiation, depending on the specific conditions and especially on the charge of the species considered, because the relative abundance of neutrals and ions may drastically change from SP to DP case. In any case, since the increase of self-absorption in DP experiments has been reported for several lines, not only resonant and not only belonging to the main element [93,94], this issue must be taken into account for any quantitative use of the spectral line intensities. If self-absorbed lines are used to build a Boltzmann plot, this may introduce a bias in the calculation of the plasma temperature: several findings of large temperature increase in DP plasmas should be critically reconsidered.

The DP enhancement observed for lines belonging to the singly and doubly-ionized species is generally higher than for neutral species [84,95,96]. In fact, double-pulse irradiation leads to plasma conditions different from the single-pulse case. Typically, the DP plasma temperature is similar or slightly higher than the SP value at the beginning of plasma evolution, then decreases more slowly. The electron density, in contrast, is often lower at the beginning of the DP plasmas evolution, but then tends to values close to those of the SP case. The number density of a species depends on the plasma temperature and electron number density according to the Saha equilibrium condition [79]:

$$\frac{n^{II}}{n^{I}} = \frac{2}{n_e}\frac{(2\pi m_e k_B T)^{3/2}}{h^3}\frac{U^{II}(T)}{U^{I}(T)}\, e^{-\frac{E_{ion}-\Delta E_{\text{ion}}}{k_B T}} \qquad 7$$

where n is the species number density, U is the partition function (superscripts refer to the ionization state: I neutral, II ionized), E_{ion} is the first ionization potential of the element under investigation, ΔE_{ion} is a correction factor due to plasma interactions, and the other symbols have already been defined. Therefore, slight variations in the plasma conditions may lead to different relative populations of the neutral and ionic species, with obvious consequences on the relative enhancement of neutral and ionic lines. In ref. [87] it has been observed that, in the spectra of the same sample, the intensity ratio of the two lines MnI 403.0 nm and MnII 294.9 nm spanned five orders of magnitude under the range of experimental conditions found during the optimization procedure (note that only inter-pulse delay and acquisition delay were varied).

The mere definition of DP enhancement is not completely exempt from ambiguities. From the analytical point of view, comparing the best signal achievable in SP mode with the best one that can be obtained in DP mode seems to make sense [14]. This implies that experimental settings must be independently optimized for the two cases [87]. However, when the aim is the comprehension of the physical phenomena at play, it does make sense to compare DP and SP spectra obtained with the same experimental settings (other than irradiation), in order to outline the different characteristics and evolution dynamics of DP and SP plasmas. Probably it should just be avoided to define the result of this comparison as an "enhancement".

In ref. [42] the intensity of some not resonant Al lines was measured in SP and DP configurations for varying laser irradiance. At low irradiance SP and DP intensities almost coincided. Above the irradiance of about 7×10^8 Wcm^{-2}, DP line intensities were at least ten times more intense than lines in SP spectra. Therefore, irradiance is a critical parameter for the evaluation of enhancement: nevertheless, DP and SP performances are always compared at the same irradiance (total or referred to the second ablative pulse). It is quite evident, however, that in this kind of comparison the enhancement will be larger or smaller depending on whether the irradiance used in SP is high enough to cause laser shielding or not. It is also worth to recall that the dependence of atomized ablated mass on the laser irradiance at ambient pressure is very steep (see Figure 1). Therefore, in describing the experimental settings, the information on pulse energy is not sufficient: fluence or irradiance are much more significant, which in turn means that a tight control of the focusing is important.

In addition, single and double-pulse plasmas follow different expansion laws. Consequently, the spatial distribution of the emitting species in the two cases is different, and the measurement of the intensity enhancement depends on the plasma region observed. This was clearly shown in ref. [97] where values of the spectral signal enhancement spanning about one order of magnitude were obtained by simply defining different spatial integration windows for the spectrally resolved images

of the plasma (later confirmed in [98]). Therefore, tight control of the detector field of view is also critical.

6. Double-pulse LIBS

In this section we undertake the description of the processes occurring during double-pulse irradiation of a solid target with ns laser beams. To this aim we make use of the concepts already introduced in the previous sections. In addition, we rely on a series of experimental results emerging from a critical inspection of the literature. We start in section 6.1 by considering the orthogonal DP configuration in pre-spark mode. In this case two laser beams are used: one is parallel to the target surface and the other perpendicular; the parallel pulse is delivered before the perpendicular one, which carries out ablation (see figure 5A). The case of the collinear DP irradiation is described in section 6.2: here, two pulses mutually delayed are focused on the target surface (figure 5B). Finally, the orthogonal re-heating mode is considered in section 6.3: also in this case two laser beams are used, one parallel and the other perpendicular to the target surface, but the perpendicular pulse (the ablating one) is delivered first (see figure 5D). For each configuration a quick overview of the processes occurring in what we consider the ideal case is provided, followed by an essential literature review that includes papers representing new advancements in the field.

6.1 Orthogonal Configuration in pre-spark mode

In this configuration the first pulse is aligned parallel to the target surface, at some distance from it, and the second is perpendicular to the target surface (figure 5 A). From a practical point of view, this configuration is more complicated than the collinear one; however, the processes occurring in this particular case are easier to understand, thanks to the clear separation between the roles played by the two pulses. We describe here what we consider the ideal orthogonal pre-spark case. First of all, the first pulse must be energetic and sharply focused enough to ignite a ionization cascade in a gas. If this is the case, the first pulse produces a plasma composed only by the elements present in

the ambient gas (no ablation of the target is produced) and an expanding shock wave that grants in front of the target a region with a rarefied gas atmosphere lasting for some microseconds or tens of microseconds, depending on its energy. The second pulse is the ablating one. It is aligned so to cross the centre of the region encompassed by the shock wave of the first pulse before reaching the target surface. If the second pulse is delivered in the optimal time interval, the ablation is enhanced because the local environmental conditions are more favourable compared to the standard atmospheric ones. In this optimal interval the low particle density in the region occupied by the first plasma plume (see section 3) reduces the shielding, so that the fraction of the second pulse energy that reaches the target is increased (see section 2.2). As a consequence, the ablated mass is increased as well, compared to the case of an ablation pulse operating in atmospheric environment. Though the focal spot of the first pulse is far enough from the sample surface that no ablation is caused, nevertheless the surface is heated by the expanding shock wave and even more, if the distance is properly chosen, by the air plasma itself. This process may also contribute to increase the ablation carried out by the second pulse (see section 4). To take advantage of the favourable environmental conditions created by the first pulse, the inter-pulse delay should be chosen large enough to allow the expanding plasma reaching the target surface (see discussion regarding fig.2). Evidently, the time needed to reach this stage of expansion depends on the laser pulse energy and wavelength, on the ambient gas density, and on the distance between the focal spot of the first laser and the sample surface.

After ablation, the plume starts expanding inside the volume of the shock wave created by the first pulse: this expansion is initially faster than the corresponding single pulse case, because of the lower gas density, and less energy is dissipated, because of the high temperature of the environment. In addition, the expansion of the ablated matter plume proceeds until it reaches the internal edge of the first pulse shock wave. When the inter-pulse delay is set to a value of the order of a μs, the first shock wave size at the time of the second pulse is of the order of a few mm. In a few hundred ns, the ablated matter plume fills this region, which is substantially larger than the

typical plume volume observed during single pulse irradiation at ambient pressure. Subsequently, the front of this expanding plume may be reflected by the shock wave internal edge and travel back toward the focal spot. The persistence of the second plume is typically longer than the single pulse case, because the shock wave generated by the first pulse acts as an insulator shell that reduces the dissipation of energy towards the external environment.

If this is the description of an ideal orthogonal pre-spark DP experiment, a not optimal combination of the experimental parameters can produce substantially different phenomena, wasting the potential advantages of the DP irradiation. In general, if the inter-pulse delay is too short, at the time of the second pulse the first plasma is still too dense and absorbs part of the photons, thus reducing the ablation efficiency. This is the mechanism exploited in the re-heating configuration: see section 6.3.

6.1.1 Pre-spark mode: literature overview

The pre-spark DP scheme was proposed in 2000 by Angel and co-workers [21, 99-100], who used two Nd:YAG lasers with fundamental wavelength for both the pre-spark and the ablation pulse. Such a configuration led to line intensity enhancement both in the case of metal targets [21] and of non-conducting targets [99]. The maximum enhancement was obtained for inter-pulse delays (Δt) ranging from 1 to 2.5 μs; however, the enhancement remained large for Δt values up to about 50 μs. An increase of plasma temperature up to 5000 K was reported for the investigated metallic samples [100] but not for glass samples [99]; an increase of crater volumes up to about 30 times with respect to SP-LIBS was found [100]. Plasma temperature and crater volume also showed a clear dependence on the inter-pulse delay, similar to that obtained for signal enhancement. The authors also noted that larger enhancements were observed for lines corresponding to transitions originating from higher energy levels; this was interpreted as an effect of the increase of plasma temperature from SP to DP configuration [100]. Another important point was raised: for large inter-pulse values, the plasma size (as resulting from time gated CCD images) was larger than the field of view of the

fibre-optic used to collect the emission. This is a possible source of artefacts in the calculated enhancements for certain experimental settings.

Gautier et al. [101] carried out DP-LIBS in pre-spark configuration on an Al target, using two Q-switched Nd:YAG lasers (λ = 1064 nm for the pre-spark and λ = 532 nm for the ablation). The largest line enhancements were obtained in an inter-pulse range going from 15 to 30 μs and for lines originating from high energy levels. Similarly to what found by Angel and co-workers, for short inter-pulse intervals (less than about 500 ns) the line intensity was found to decrease. Hohreiter and Hahn also found that using an ablating 532 nm pulse in combination with a simultaneous ($\Delta t=0$) air spark lowers the performance with respect to the ablating pulse alone [86]. These observations can be explained by taking into account the evolution in time of plasma transmissivity as measured by Hohreiter et al. [102]. They showed that the laser-induced plasma is initially opaque to visible or infrared light and gradually becomes more transparent until it reaches complete transparency (with their experimental condition, this was at about 500 ns from the pulse).

In their paper, Gautier et al. proposed a procedure to represent the changes in spectral intensity between single and double-pulse case as a function of plasma temperature and emitter number density [101]. Though based on some rough simplifications, the use of the procedure evidenced that the intensities variation observed in their measurement were due to changes in the plasma temperature. In 2012, Hahn and Omenetto presented a similar approach, with a separated treatment for neutral and ionic lines, and with the addition of a final step: the representation of the spectral data in a bi-logarithmic plot [14]. This further step makes clear the separation of the effects of changes in the plasma temperature (that can be measured from the slope of the plot) and changes in the ablated mass (that can be obtained from the intercept).

The influence of the distance (d) between the pre-spark focal spot and the surface of a brass target was studied in ambient air, using spectroscopic and shadowgraphic approaches, in ref. [66]. The laser sources were two Nd:YAG lasers emitting at 1064 nm. The spectra of the air spark did not evidence a detectable emission from target species even in the closest case of d = 0.1 mm. Spectra

were acquired at a fixed delay from the ablation pulse, while the inter-pulse delay was varied. For increasing values of the distance *d*, the signal enhancement started at progressively higher inter-pulse delay times. The inspection of the shadowgraphic images of the plasma, showing the evolution of the shock waves produced by the two laser pulses, revealed their strong dependence on the combination of values of the parameters *d* and Δt. If the ablation laser is fired before that the shock wave SW1 generated by the air spark arrives on the target surface, the ablation plume and the shock wave SW2 expand mainly in the lateral direction, assume a flat shape similar to a disc and do not coalesce with the air spark. No improvement of the ablation efficiency is observed in this case, nor signal enhancement. The most unfavourable condition is when the second pulse is delivered at the time the SW1 reaches the target surface, because the high density gas layer at the shock front results in a strong shielding of the laser pulse and reduces the ablation efficiency. In the measurements carried out at different values of the inter-pulse delay, this condition was detected as a reduction of the signal at values of Δt immediately before the onset of signal enhancement. On the contrary, if the ablation pulse is fired well after the time taken by SW1 to reach the target, the ablation is made easier by the presence of the rarefied region created by the first plume. In this condition, SW1 and SW2 become almost concentric and the two plumes rapidly coalesce. The largest signal enhancement was obtained when the distance *d* was less than 1 mm [66]. The same behaviour was observed by Sanginés et al. [74], who attributed the DP enhancement to the increased amount of ablated material, favoured by the target surface heating due to the pre-spark. The DP enhancement as a function of the laser fluence was investigated in [54], by comparing the signals obtained in SP and pre-spark DP with the ablating pulse at the same fluence. The highest enhancement values where observed in the fluence range that, under SP irradiation and at atmospheric pressure, leads to the onset of the LSD regime, so that the laser shielding makes the phase explosion mechanism less efficient. In DP case, instead, due to the reduced particles density, a larger fraction of the laser energy reaches the target surface and phase explosion is able to give

strong ablation. The study of the crater morphology suggested that in DP configuration melt displacement and splashing is less effective than in SP at the same fluence.

Lindner et al. [103] compared the size distribution of the clusters generated in SP and in pre-spark DP laser ablation in argon (brass target, $\lambda = 1064$ nm). They found that the DP irradiation shifted the distribution toward a predominance of ultrafine particles (< 50 nm). Since ultrafine particles are generated by vapour-phase condensation during plasma cooling (while large clusters are produced during the mass removal stage), the authors conclude that the DP scheme provides a better atomization of the ablated matter. According to the authors, thus, the signal emission enhancement in pre-spark configuration is produced by the increase of both the ablated mass and its atomization. Larger ablation is also accompanied by lower re-deposition of sample material in and around the crater, another effect of the reduced gas density.

Another experimental parameter that should be taken into account is the laser repetition frequency. In a subsequent work, in fact, Lindner et al. [104] found out that a repetition rate of 5 Hz in DP pre-spark configuration provided not only high signal enhancement but also good values of the relative standard deviation, contrarily to the case of experiments carried out at a repetition rate of 0.6 Hz, that were characterized by high fluctuations. This behaviour was explained as an effect of the persistence of particles ablated by the preceding pulses in the focal area of the parallel beam, in front of the sample, which absorb part of the parallel pulse energy by Mie absorption (see section 2.1). At higher repetition rate, in fact, the higher density of remaining particles improves the coupling of the parallel pulse in the resulting air plasma, giving the same result that could be obtained in a pure gaseous environment with a more energetic pulse.

6.2 Collinear configuration

Reports on collinear DP irradiation (figure 5 B) are much more abundant in the literature than reports based on the orthogonal configuration. In some cases two lasers are used to implement the

collinear DP arrangement and in other cases two or more pulses are delivered from a single laser during the flashlamp pumping time. Very briefly, the advantage of using two lasers is a greater flexibility while the advantage of using just one laser is an easier alignment and therefore a greater stability.

Configurations where the laser beams hit the target at non-normal angles of incidence (figure 5 C) have also been described (see for example ref. [105], and ref. [106] for standoff measurements). However, both the laser pulses produce ablation of the sample and the second one benefits of the favourable environmental conditions created by the first pulse: thus, the physical processes at play are similar to those occurring in the collinear configuration with two beams aligned perpendicularly to the target surface. Therefore, the description proposed in this section applies also to such cases. The same applies to plasmas obtained by multiple (more than two) collinear pulses separated by intervals of the order of a μs (see for example ref. [88]).

We start again the section by describing what we consider the ideal collinear DP case. In this configuration both laser pulses are aligned perpendicularly to the target surface and both produce ablation. However, the mass ablated by the first pulse is typically much less than the mass ablated by the second pulse. By using a rough simplification, we can say that the first pulse negligibly contributes to the total ablated mass, while it substantially affects the environmental conditions of the interaction between the second pulse and the target surface. In this sense, the collinear configuration can be seen as an extreme case of the orthogonal one, where the distance between the pre-spark and the target surfaces tends to zero. In fact, the first pulse causes on the one hand a temporary rise of the target surface temperature, on the other hand the formation of a plasma plume and shock wave that produce a transient change in the local atmospheric conditions (see section 3). If a suitable value of the inter-pulse delay is chosen, these two effects cooperate to increase the coupling of the second pulse energy with the target surface, so that the total mass ablated is larger than in the case of a single pulse of the same total energy. It is difficult to quantify the relative contributions of target temperature and ambient rarefaction to increase ablation efficiency; to our

knowledge no one work in the literature did achieve this quantification. However, some experimental results suggest that the effect of the increased target temperature is not dominant [107]. In addition, the plume produced by the second pulse expands in the rarefied and heated environment internal to the shock wave, dissipating less energy than in the unperturbed atmospheric case and resulting in a longer persistence. The separation of the two effects of increased ablation and higher plasma temperature on the spectral line enhancement is possible and has been in fact proposed by Gautier et al. [101] and Hahn and Omenetto [14] (see section 6.1.1). The application of their methods reveal that depending on the material investigated and on the experimental conditions any of the two factors may be predominant.

A signal enhancement is obtained under collinear DP irradiation if the inter-pulse delay is chosen within a suitable interval, typically ranging from about 1 to a few tens microseconds (but it depends on the actual experimental settings). Similarly to what already mentioned in section 6.1 for the pre-spark configuration, when the inter-pulse delay is less than about 500 ns the result is often a decrease of the spectral signal and of the ablated mass, and an increase of the continuum radiation intensity. This is due to the fact that the plasma ignited by the first pulse has not been allowed to expand yet, and the high density of particles in the shock wave front, still in proximity of the focal volume, intercepts and absorbs a great fraction of the second pulse energy. However, the signal enhancement obtained under DP irradiation also depends on the characteristics of the target. In fact, the line intensity depends on the amount of mass ablated (which is related to the mechanisms of mass removal from the target, and, in turn, to the material and ambient gas properties) and on the thermodynamic parameters of the plasma, e.g. temperature and electron density (which are related to the ignition process of the plasma and to its dynamical evolution). This issue is discussed in the final part of the next sub-section.

6.2.1 Collinear configuration: literature overview

The collinear configuration was explored since 1969, when the pioneering studies by Piepmeier and Malmstadt and Scott and Strasheim (1970)[1,108] mentioned the enhancement of the plasma spectral emission obtained by multi-spike irradiation. Then, Maher and Hall in 1976 published the first work completely dedicated to the study of the effects of collinear double-pulse irradiation [109]. Though they used two CO_2 lasers, the conclusions they draw are the same that have been proposed again after decades by researchers using ns DP. Maher and Hall stated that enhanced laser-target coupling might be expected if a second laser pulse is delivered to the target while the ambient conditions are still modified by the effect of the first pulse: namely, while the gas density is reduced due to the presence of an expanding shock wave. In addition, the increase in the surface temperature produced by the first pulse persists for a relatively long time, and the surface reflectivity found by the second pulse may be different from the unperturbed case. In his ns DP experiments, carried out in the late eighties, Pershin [18] observed a suppression of the emission by atmospheric gases, and explained it as a consequence of a reduced density of air in the interaction region at the moment of arrival of the second pulse. These results were later confirmed by Colao et al. [22].

According to St-Onge et al., the plasma produced by DP irradiation is not much hotter or denser than that formed after a single pulse [110]. The spectral intensity enhancement can be explained by a larger emitting volume, a region where the optimal temperature for emission is maintained for a longer time, because of the lower thermal conduction losses toward the sample and lower radiation losses toward the environment, as a consequence of the expanding plasma already present at the time of the second pulse. A larger high temperature volume in double-pulse plasmas was observed indeed by Corsi et al. after Abel inversion of spatially resolved spectral measurements of plasma emission [91].

While the above mentioned studies used for irradiation two or more pulses of the same wavelength, mostly infrared pulses from a Nd:YAG laser, St-Onge et al. proposed a DP setup exploiting the

combination of the fundamental and fourth harmonic of a Nd:YAG laser [111], with the aim of separating the two steps of sampling and excitation, and using the most appropriate laser wavelength for each one. The explanation of the high intensity enhancements found in this experiment is based on the different efficiency of inverse bremsstrahlung absorption for the two wavelengths (see section 2). The increased plasma temperature (due to improved excitation efficiency of the ablated matter in the plasma core) was found to account for most of the enhancement. The remaining part was attributed to the larger emitting volume and increased ablation (as apparent from the increased crater depth). By inspecting the behaviour of several spectral lines, the authors noted a correlation between the enhancement and the upper level energy of the transition, and also different optimal inter-pulse delays for the enhancement of neutrals and ions [111]. These observations were later confirmed by Gautier et al. [84]. The work by Benedetti et al. investigated the effect of the first pulse energy in the DP configuration at different inter-pulse delays varying between 0 and 50 μs [112]. In this experiment the increase in the mass removed in DP was found to explain the bulk of the spectral intensity enhancement, while the slight temperature increase explained the trend of enhancement with the upper level energy of the transition.

Petukh et al. compared the intensities of several spectral lines obtained under SP and DP conditions at different buffer gas pressure values and for increasing distance from the target surface, observing different spatial distributions of the emitters between SP and DP plasmas [113]. Since they found a close correspondence between the DP intensity at atmospheric air pressure and the SP intensity at a pressure of 200 mm Hg, they extrapolated that in the plasma of the second laser pulse the air density is about four times smaller than in the plasma of single pulses. As an order of magnitude, this result is in agreement with calculations carried out in ref. [67]. Later, Cristoforetti et al. found out that DP irradiation produces a signal enhancement (for species ablated from the target) only for ambient pressure values higher than about 100 torr [79]. In fact, in a lower ambient gas pressure, the additional transient rarefaction due to the first shock wave makes the gas density lower than the

optimal value for a single pulse ablation, i.e. produces conditions where ablation is further enhanced but expansion is too fast and plasma temperature too low to sustain spectral emission. In addition, the authors measured electron number density and temperature under SP and DP irradiation for several values of the ambient gas pressure and of the inter-pulse delay, and showed how the interplay of the plasma parameters explains the different behaviour observed for the enhancement of neutrals and ions.

Colao et al. measured the plasma ignition threshold for the second pulse of a DP pair, in dependence on the inter-pulse delay and on the irradiance of the first pulse [114]. A strong reduction of the ignition threshold was observed for the inter-pulse delay of 38 μs; when increasing the irradiance of the first pulse, the reduction of the threshold became evident also for greater inter-pulse delays.

In their shadowgraphic investigation of the expansion law of single- and double-pulse plasmas, Corsi et al. found that the shock wave produced by the first pulse continues its expansion independently of the delivery of a second pulse. On the contrary, the plasma initiated by the second pulse expands much more rapidly, until it reaches the first shock front [91]. Noll et al. also studied the evolution of single and double-pulse plasmas in air using a streak camera [23]. They observed that the plasma created by the single pulse stays in contact with the sample surface and its size expands to about 1 mm above the sample. The expansion dynamics of the second pulse plasma is much more complicated: starting again from the sample surface, it expands up to a distance of about 2 mm, until it inverts its direction after 300 ns, propagating back towards the sample. After reaching again the sample surface approximately 600 ns after the irradiation, the plasma front is partially reflected. The observed inversion of the direction of the luminous front at about 300 ns after the second laser pulse can be explained, in the framework of the Sedov theory of strong explosion, by the presence of a radially increasing particle density coincident with the front of the first pulse shock wave [23]. The plume reflection described by Noll et al. has been observed also by Cristoforetti et al. [97] by means of time resolved imaging of DP plasmas expansion at different

values of the ambient pressure and for different values of the inter-pulse delay. Depending on the experimental conditions, the plume oscillation (expansion from the focal spot volume on the target surface up to the internal layer of the shock front and then contraction after reflection by the internal layer of the shock front) may be repeated for several cycles until the kinetic energy of the plume is almost completely dissipated. This was clearly observed at a pressure of 1.3×10^4 Pa, for inter-pulse delays of 0.7, 2 and 5 μs [97].

Mao et al. [24] investigated in greater detail the inter-pulse range between 1 ns and 1 μs by irradiating a silicon target. They found that spectral emission, plasma temperature and particle number density decrease for inter-pulse values up to 100 ns, then abruptly increase for Δt = 200 ns and tend to decrease again approaching Δt = 1 μs. The plasma images revealed that for Δt = 100 ns the second pulse is strongly absorbed by the expanding front of the shock wave created by the first pulse, which at that time is characterized by high density, so that the energy doesn't contribute to feed the main plasma at the target surface. At later times, the expansion has reduced the local density of the shock front, so that the second pulse is not blocked at its surface. The measurement of the crater profile confirms this view [24].

Among the possible mechanisms responsible of the signal enhancement in double-pulse, some works point to the heating of the sample surface, produced by the first pulse, that would make the subsequent ablation easier. This applies especially to cases where one of the two pulses is from a CO_2 laser [115]. Krstulovic and Milosevic interpreted the larger ablation rate in DP in vacuum as a consequence of decreased reflectivity of the target surface due to its increased temperature. This interpretation is in agreement with the discussion on enhancement with repetition-rate (see section 4) [80]. It must be considered, however, that the enhancement observed under DP irradiation as a function of the repetition rate may also be due to the persistence in the laser focal volume of particles ablated from the preceding shots. These particles may play a role in increasing the energy of the first pulse plasma through Mie absorption of the laser photons [104].

Several groups investigated the dependence of line enhancement on the matrix. Gautier et al. [116] investigated aluminium, steel, glass and rocks and found out that in DP the temperature in some cases increased (aluminium and vitreous matrices), in some other cases decreased (steel). Increased ablation efficiency was observed only for some samples (glass, rocks and steel). However, different behaviours have also been observed for aluminium alloys and steel, as reported in the literature [87]. In a more systematic study [57], the emission enhancement of neutral and ionic lines from several pure metal targets was measured: low enhancement was observed for the lines of Pb, Ni and Mn targets and high enhancement for Cu, Al and Au. High values of ablated mass enhancement were correlated with high values of the thermal diffusivity. Thermal diffusivity plays a fundamental role in determining the phase explosion threshold of materials irradiated: the higher the thermal diffusivity of the metal, the higher the irradiance needed to reach the boiling explosion regime. In SP irradiation, where the effective irradiance is lowered due to the plasma shielding, a larger ablation of matter is expected for the lower thermal diffusivity metals, which more easily reach the boiling explosion regime. In the DP configuration, instead, a much larger fraction of the second pulse energy reaches the target, thereby overcoming the boiling explosion threshold also for the metals with high thermal diffusivity. In this case, the larger depth of the molten pool characteristic of the metals with high thermal diffusivity may be the determinant factor in increasing the amount of material expelled [57].

6.3 Orthogonal configuration in re-heating mode

In the re-heating mode, the order of pulses delivery is the reverse than in the case of pre-spark (see section 6.1). In fact, a first laser pulse is perpendicularly directed on the sample surface to produce ablation; after a suitable delay, a second laser beam, with its axis parallel to the sample surface, is directed through the pre-existing plasma, avoiding any interaction with the sample surface (figure 5 D). The most common feeling about this configuration is that it produces a relatively small enhancement in the emission intensity compared to the case of a single ablating pulse (however, the

related literature is not in agreement on this point - see below). To obtain a detectable plasma reheating, the second laser pulse must be at least in part absorbed by the plasma produced by the first laser pulse. To this aim, the particular combination of settings of the two laser pulses is crucial. The wavelength of the second pulse is one of the main parameters influencing the effectiveness of the reheating. As shown in section 2, inverse bremsstrahlung is the dominant mechanism for absorption of infrared wavelengths, while photoionization is dominant for UV wavelengths, even though Mie absorption may also be present. Overall, infrared wavelengths seem to result in higher absorption in typical LIBS plasmas (see section 2.2).

The inter-pulse delay is the other important parameter: as discussed in section 2, the absorption coefficients are proportional to the density of the particles involved. Especially ion density seems to play an important role. Considering that the radius of the shock wave, in the spherical geometry, scales as $t^{0.4}$ and that the particle density, in a first approximation, decreases like the reciprocal of the plasma volume, it is evident that stronger absorption is expected for short values of the inter-pulse delay. The interval of inter-pulse delays that yields the highest line enhancement in the orthogonal pre-spark mode doesn't yield signal enhancement in the orthogonal re-heating mode, and vice versa. In fact, in pre-spark mode, at the time of delivery of the second pulse, the first plasma density must be low enough to allow the second pulse energy reaching the target surface and ablating more matter than in an unperturbed atmospheric environment. In re-heating mode, instead, at the time of delivery of the second pulse the first plasma density must be as high as possible to efficiently absorb its energy. It is not possible to define a specific value of the inter-pulse delay as the boundary between the range optimal for re-heating and the range optimal for pre-spark mode, because it depends on the combination of experimental settings. In ref. [102] the time needed for the plasma to become substantially transparent to incident radiation is about 500 ns.

The experimental cost of an orthogonal arrangement has to be counterbalanced by substantial advantages in the analytical performance. This is probably the reason why this configuration is not very frequently implemented and the earlier feasibility studies that are found in the literature have

been devoted to very specific objectives. For example, plasma re-heating allowed experimentalists obtaining detectable signals also when using very low energy ablation pulses (to reduce the superficial damage) or after long delays from plasma ignition (to wait for a complete atomization of the ablated particles or to improve the spectral resolution thanks to the linewidths narrowing with time). Another particular case of re-heating has been implemented where the second pulse wavelength is tuned to a resonant transition of the matrix element in the sample. These cases are briefly discussed in the next section.

6.3.1 Re-heating mode: literature overview

The re-heating mode was proposed by Niemax and co-workers in 1991 [19]. The aim of these authors was indeed the enhancement of line emission, but in the special case of a plasma that was allowed to cool down for 40 μs in order to achieve the complete atomization of the material ablated by the first pulse. The second pulse was then aligned parallel to the sample surface, at a distance of 1.5 mm from it, and focused in correspondence of the first plasma. The experiment was carried out in Ar atmosphere at 200 hPa, using two 1064 nm pulses for both ablation and reheating. The temperature after the second pulse was measured and a detectable re-heating was found, even though the plasma didn't reach the temperature values corresponding to its initial stages. In addition, the decay of the temperature after the second pulse was steeper than after the first pulse. Due to these conditions, the intensity of a Mn neutral line in a steel sample, after reheating, did not ever reach the values observed in the early stages of the single ablation plasma. Therefore, strictly speaking, no line enhancement was observed. The authors actually claim a tenfold enhancement of the Cu and Zn lines in brass, because they compare the spectral intensities measured 2 μs after the re-heating pulse with the corresponding intensities measured 40 μs after the ablating pulse. However, the point was to obtain a measurable signal at late times of the plasma evolution. According to this work, the opportunity of carrying out emission measurements after the complete atomization of the material contained in the plasma is an advantage in the analysis of materials

whose components have very different values of the vapour pressure, such as brass, and also in the analysis of materials for which standards are not available. In fact, the complete atomization of the ablated matter allows the exploitation of internal standardization, and the preparation of calibration curves independent of the matrix.

In 2000, Stratis et al. explored the potential of the orthogonal double-pulse arrangement by measuring the variation of the signal to background ratio in dependence of the inter-pulse delay [21]. Their settings spanned from pre-ablation to re-heating mode. For the two elements (Pb and Cu) and the two neutral lines chosen for the measurement, no improvement of the signal to background ratio could be observed in re-heating mode compared to the single pulse case. No information was provided on the separate behaviour of line intensity and background intensity in the re-heating mode. Though the experimental conditions were different (in this case measurements were carried out in atmospheric environment; pulse energy values were also different), these results are not in contrast to what shown in ref [19].

A subsequent work by Gautier et al. was especially focused on the potential of re-heating for signal enhancement [92]. Two findings need to be mentioned: the dependence of the line intensity enhancement on the inter-pulse delay and the different behaviour of neutral and ionic lines. Regarding the first point, this study pointed out that only inter-pulse delays lower than about 0.5 μs are able to produce a detectable increase of the spectral lines intensity (in particular for the ionic lines). The authors hypothesized that at high inter-pulse delays the plasma may be too much expanded and the electronic density too low to reabsorb the energy of the second pulse. In addition, Gautier et al. observed that neutral and ionic lines generally show an opposite enhancement behaviour. At the optimal inter-pulse delay of 200 ns, ionic lines are enhanced while the intensity of neutral lines is reduced. This is possibly explained by recalling that the second pulse doesn't produce ablation, and the number of atoms of a given element can be considered constant in the detector field of view during a given interval of observation. Clearly, the temperature increase caused by the second pulse shifts the balance between the population of the neutral and ionic

species toward the ionic ones. The population of the higher excited levels is also increased with a larger coefficient. However, in their following work [101] the authors warned that a mechanism of spatial selection may also had occurred, since the signal was acquired only from the central region of the plasma where ionic lines are generally more intense than neutral lines.

In the subsequent years, papers were published reporting enhancement of the spectral line intensity also for re-heating pulses delivered after delays of some μs from the ablation pulse. In 2010 Oba et al. [117] carried out an investigation similar to the one already reported by Stratis et al. in ref [21], where the effect of the inter-pulse delay on spectral line intensity was studied, and the results were not in agreement. In ref. [21], the pre-spark configuration originated strong improvement of the signal to noise ratio while the re-heating was not beneficial compared to the single pulse; in ref. [117], instead, the re-heating increased the line intensity by up to 25-fold, while the pre-spark mode was not beneficial compared to the single pulse ablation. However, it must be considered that all the experimental settings (pulse energy and wavelength, collection geometry, observation time, etc.) were different in the two cases. This work confirmed however that ionic line intensity in re-heating configuration is subjected to a greater enhancement than neutral line intensity. Mao et al. also observed an increased signal intensity by associating the ablation pulse to a second re-heating pulse delayed by 2.4 μs [118]. Guo et al. combined the orthogonal double-pulse in re-heating configuration with a pair of confinement walls to exploit the enhancement potential provided by the two techniques [119]. They found out that an inter-pulse delay of 25 μs produced the maximum line intensity enhancement for a Cr resonant neutral line.

Choi et al. reported eight-fold enhanced emission for a Mg II line using 1μs delayed double-pulse excitation in comparison to the single-pulse case. The enhanced emission was accompanied by a narrower linewidth, as a consequence of a lowered electron density by the use of double-pulse LIBS [120].

A different re-heating approach (Resonance-Enhanced LIBS or RELIPS) was proposed by Cheung and co-workers. To minimize the surface damage they used a low fluence (about 1 J cm^{-2}) ablation

pulse followed by a second laser pulse after about 30 ns. The wavelength of the second pulse (from a dye laser) was tuned to resonantly excite the most abundant component of the sample matrix. The excitation energy of the target species was subsequently thermalized via electron collisions, so that the plasma temperature was high enough for spectral detection of the wanted analyte for a longer time [121]. The arrangement of the two pulses could be orthogonal or not [122], but in this second case the fluence of the second pulse was lower than the ablation threshold. According to Cheung and co-workers, the RELIPS enhancement originates from the larger volume of the plasma that is re-heated by the resonant pulse, in comparison to the non-resonant re-heating case, where the inverse Bremsstrahlung process tends to selectively heat the hot spots in the plasma, characterized by a large electron density [123]. Hahn and Omenetto pointed out that a direct energy transfer between the atoms of the matrix and those of the trace elements does not seem a favourable route, while it is plausible that it is mediated by the more energetic electrons, formed after the resonance saturation of the lines of the matrix element [14, page 381]. Goueguel et al. confirmed the possibility of improving LODs using RELIBS compared to the case of single pulse LIBS with the same ablation energy [124].

Conclusions

In this paper we proposed an interpretation of the main mechanisms at play during ns DP-LIBS of solid samples in gas environment. Though the interpretation is not new, we made an effort to support it as firmly as possible, in order to convince all those researchers who asserted that the reasons of the DP signal enhancement have not been understood yet. We are convinced that, if confusion exists, it has been caused by the will of giving a unique explanation to processes too different from each other, which only share the number of pulses used for irradiation and nothing else. Thus, we selected a homogeneous set of experimental conditions, characterized by ns laser pulses, solid samples, gaseous environment. Then, we recalled some phenomenological aspects of a ns laser-induced plasma, in order to make clear the differences existing between the conditions of

the unperturbed buffer gas and those at the centre of a plasma. Finally, we considered three possible arrangements to combine the two ns pulses: orthogonal pre-spark, collinear, orthogonal re-heating. The first two arrangements can be considered quite similar: in both cases the main ablating pulse is the second one, and the first (parallel or perpendicular to the target, it doesn't change so much) is "only" needed to create favourable conditions for ablation. The advantages typically obtained with respect to a SP are: larger ablated mass, larger atomized mass, higher plasma temperature, larger emitting volume, longer emission persistence. It would be reasonable to expect also a more homogeneous plasma and conditions more close to local thermodynamic equilibrium (LTE), at least after the first stage of rapid expansion (i.e. after the volume of the first shock wave has been filled by the plume of the second pulse). However, to our knowledge, this topic is still waiting for careful investigation.

The orthogonal re-heating case is completely different, because the first pulse is the ablating one: since ablation is carried out in the unperturbed buffer gas conditions, no increase of ablated mass with respect to SP can be expected, of course. Nevertheless, if the coupling between the second pulse and the ablated plume is efficient, the atomized ablated mass, the plasma temperature and the emitting volume can be increased with respect to SP, so that a signal enhancement may be obtained as well. This configuration, however, seems to be especially suited for some kind of niche investigation. For a quick reference, the main characteristics of the different configurations described in this paper are briefly summarized in Table I.

By compiling this review we didn't mean to send the message that everything is already known about ns double pulse on solid samples. We just wanted to raise some points that may serve as references for new investigations. It may be useful to stress once again that the highest control of the experimental apparatus means the highest significance of the measurement results.

References

1 E.H. Piepmeier, H.V. Malmstadt, Q-Switched Laser Energy Absorption in the Plume of an Aluminum Alloy, *Anal. Chem.*, 1969, **41**, 700-707.

2 J. González, C. Liu, J. Yoo, X. Mao, R. E. Russo, Double-pulse laser ablation inductively coupled plasma mass spectrometry, *Spectrochim. Acta Part B*, 2005, **60**, 27-31.

3 M. Miclea, C.C. Garcia, I. Exius, H. Lindner, K. Niemax, Emission spectroscopic monitoring of particle composition, size and transport in laser ablation inductively coupled plasma spectrometry, *Spectrochim. Acta Part B*, 2006, **61**, 361-367.

4 A.C. Forsman, P.S. Banks, M.D. Perry, E.M. Campbell, A.L. Dodell, M.S. Armas, Double-pulse machining as a technique for the enhancement of material removal rates in laser machining of metals, *J. Appl. Phys.*, 2005, **98**, 033302.

5 S. Witanachchi, K. Ahmed, P. Sakthivel, P. Mukherjee, Dual-laser ablation for particulate-free film growth, *Appl. Phys. Lett.*, 1995, **66**, 1469-1471.

6 G. Cristoforetti, V. Palleschi, Double-pulse laser ablation of solid targets in ambient gas: mechanisms and effects, in *Laser ablation: effects and applications*, Ed. S.E. Black, Nova Science Publishers, Inc., New York, 2011. ISBN 978-1-61122-466-5.

7 J. Pender, B. Pearman, J. Scaffidi, S.R. Goode, S.M. Angel, Laser-induced breakdown spectroscopy using sequential laser pulses, in *Laser-induced breakdown spectroscopy: fundamentals and applications*, Eds. A.W. Miziolek, V. Palleschi, I. Schechter, Cambridge University Press, New York, 2006. ISBN-13 978-0-521-85274-6.

8 R. Noll, *Laser-Induced Breakdown Spectroscopy: Fundamentals and Applications*, Springer, Berlin, 2012. ISBN 3-642-20667-0.

9 L.J. Radziemski, D.A. Cremers, *Handbook of laser-induced breakdown spectroscopy*, John Wiley, New York, 2nd edn., 2013. ISBN 978-1-118567364.

10 A. De Giacomo, M. Dell'Aglio, D. Bruno, R. Gaudiuso, O. De Pascale, Experimental and theoretical comparison of single-pulse and double-pulse laser induced breakdown spectroscopy on metallic samples, *Spectrochim. Acta Part B*, 2008, **63**, 805-816.

11 V.I. Babushok, F.C. De Lucia jr, J.L. Gottfried, C.A. Munson, A.W. Miziolek, Double pulse laser ablation and plasma: Laser induced breakdown spectroscopy signal enhancement, *Spectrochim. Acta Part B*, 2006, **61**, 999-1014.

12 J. Scaffidi, S.M. Angel, D.A. Cremers, Emission enhancement mechanisms in dual-pulse LIBS, *Anal. Chem.*, 2006, **78**, 24-32.

13 A. De Giacomo, M. Dell'Aglio, O. De Pascale, M. Capitelli, From single pulse to double pulse ns-Laser Induced Breakdown Spectroscopy under water: Elemental analysis of aqueous solutions and submerged solid samples, *Spectrochim. Acta Part B*, 2007, **62**, 721-738.

14 D.W. Hahn, N. Omenetto, Laser-Induced Breakdown Spectroscopy (LIBS), Part II: Review of instrumental and methodological approaches to material analysis and applications to different fields, *Appl. Spectrosc.*, 2012, **66**, 347-419.

15 G. Cristoforetti, M. Tiberi, A. Simonelli, P. Marsili, F. Giammanco, Toward the optimization of double-pulse LIBS underwater: effects of experimental parameters on the reproducibility and dynamics of laser-induced cavitation bubble, *Appl. Opt.*, 2012, **51**, B30-B41.

16 B.C. Windom, P.K. Diwakar, D.W. Hahn, Dual-pulse laser induced breakdown spectroscopy for analysis of gaseous and aerosol systems: plasma-analyte interactions, *Spectrochim. Acta Part B*, 2006, **61**, 788–796.

17 N. Krstulović, N. Čutić, S. Milošević, Cavity ringdown spectroscopy of collinear dual-pulse laser plasmas in vacuum, *Spectrochim. Acta Part B*, 2009, **64**, 271–277.

18 S.M. Pershin, Physical mechanism of suppression of the emission of radiation by atmospheric gases in a plasma formed as a result of two-pulse irradiation of the surface, *Sov. J. Quant. Electron.*, 1989, **19**, 1618-1619.

19 J. Uebbing, J. Brust, W. Sdorra, F. Leis, K. Niemax, Reheating of a laser-produced plasma by a second pulse laser, *Appl. Spectrosc.*, 1991, **45**, 1419-1423.

20 L. St-Onge, M. Sabsabi, P. Cielo, Analysis of solids using laser-induced plasma spectroscopy in double-pulse mode, *Spectrochim. Acta Part B*, 1998, **53**, 407-415.

21 D.N. Stratis, K.L. Eland, S.M. Angel, Dual-pulse LIBS using a pre-ablation spark for enhanced ablation and emission, *Appl. Spectrosc.*, 2000, **54**, 1270-1274.

22 F. Colao, V. Lazic, R. Fantoni, S. Pershin, A comparison of single and double pulse laser-induced breakdown spectroscopy of aluminum samples, *Spectrochim. Acta Part B*, 2002, **57,** 1167-1179.

23 R. Noll, R. Sattmann, V. Sturm, S.J. Winkelmann, Space- and time-resolved dynamics of plasmas generated by laser double pulses interacting with metallic samples, *J. Anal. At. Spectrom.*, 2004, **19**, 419-428.

24 X. Mao, X. Zeng, S.B Wen, R.E. Russo, Time-resolved plasma properties for double pulsed laser-induced breakdown spectroscopy of silicon, *Spectrochim. Acta Part B*, 2005, **60**, 960-967.

25 Y. Iida, Effect of atmosphere on laser vaporization and excitation processes of solid samples, *Spectrochim. Acta Part B*, 1990, **45,** 1353-1367.

26 W. Sdorra, K. Niemax, Basic investigations for laser microanalysis: III. Application of different buffer gases for laser-produced sample plumes, *Mikrochim. Acta*, 1992, **107**, 319-327.

27 G. Cristoforetti, G. Lorenzetti, S. Legnaioli, V. Palleschi, Investigation on the role of air in the dynamical evolution and thermodynamic state of a laser-induced aluminium plasma by spatial- and time-resolved spectroscopy, *Spectrochim. Acta Part B*, 2010, **65**, 787-796.

28 A. De Giacomo, M. Dell'Aglio, R. Gaudiuso, S. Amoruso, O. De Pascale, Effects of the background environment on formation, evolution and emission spectra of laser-induced plasmas, *Spectrochim. Acta Part B*, 2012, **78**, 1-19.

29 R.E. Russo, X.L. Mao, J.J. Gonzalez, V. Zorba, J. Yoo, Laser Ablation in Analytical Chemistry, *Anal. Chem.*, 2013, **85**, 6162−6177.

30 S. Amoruso, R. Bruzzese, N. Spinelli, R. Velotta, Characterization of laser-ablation plasmas, *J. Phys. B*, 1999, **32**, R131–R172**.**

31 R.E. Russo, X.L. Mao, S.S. Mao, The Physics of Laser Ablation in Microchemical, *Anal. Chem.*, 2002, **74**, 70A−77A.

32 G. Cristoforetti, E. Tognoni, L.A. Gizzi, Thermodynamic equilibrium states in laser-induced plasmas: From the general case to laser-induced breakdown spectroscopy plasmas, *Spectrochim. Acta, Part B*, 2013, **90**, 1 – 22.

33 G. Cristoforetti, S. Legnaioli, V. Palleschi, E. Tognoni, P.A. Benedetti, Observation of different mass removal regimes during the laser ablation of an aluminium target in air, *J. Anal. At. Spectrom.*, 2008, **23**, 1518-1528 and Corrections, *J. Anal. At. Spectrom.*, 2009, **24**, 1684-1684.

34 A. Bogaerts, Z.Y. Chen, Effect of laser parameters on laser ablation and laser-induced plasma formation: A numerical modeling investigation, *Spectrochim. Acta, Part B*, 2005, **60**, 1280 – 1307.

35 A. Bogaerts, Z.Y. Chen, D. Bleiner, Laser ablation of copper in different background gases: comparative study by numerical modeling and experiments, *J. Anal. At. Spectrom.*, 2006, **21**, 384-395.

36 A.E. Hussein, P.K. Diwakar, S.S. Harilal, A. Hassanein, The role of laser wavelength on plasma generation and expansion of ablation plumes in air, *J. Appl. Phys.*, 2013, **113**, 143305.

37 R. Rozman, I. Grabec, E. Govekar, Influence of absorption mechanisms on laser-induced plasma plume, *Appl. Surf. Sci.*, 2008, **254**, 3295–3305.

38 H. Schittenhelm, G. Callies, A. Straub, P. Berger, H.Hugel, Measurements of wavelength-dependent transmission in excimer laser-induced plasma plumes and their interpretation, *J. Phys. D*, 1998, **31**, 418–427.

39 D. Breitling, H. Schittenhelm, P. Berger, F. Dausinger, H. Hügel, Shadowgraphic and interferometric investigations on Nd:YAG laser-induced vapor/plasma plumes for different processing wavelengths, *Appl. Phys. A*, 1999, **69**, S505–S508.

40 D. Marla, U.V. Bhandarkar, S.S. Joshi, Critical assessment of the issues in the modeling of ablation and plasma expansion processes in the pulsed laser deposition of metals, *J. Appl. Phys.*, 2011, **109**, 021101.

41 Q.L. Ma, V. Motto-Ros, F. Laye, J. Yu, W.Q. Lei, X.S. Bai, L.J. Zheng, H.P. Zeng, Ultraviolet versus infrared: Effects of ablation laser wavelength on the expansion of laser-induced plasma into one-atmosphere argon gas, *J. Appl. Phys.*, 2012, **111**, 053301.

42 G. Cristoforetti, G. Lorenzetti, P.A. Benedetti, E. Tognoni, S. Legnaioli, V. Palleschi, Effect of laser parameters on plasma shielding in single and double pulse configurations during the ablation of an aluminium target, *J. Phys. D*, 2009, **42**, 225207**.**

43 R.G. Root, Modeling of post-breakdown phenomena, in *Laser-induced Plasmas and Applications*, Eds. L.J. Radziemski, A. Cremers, Marcel Dekker, New York, 1989.

44 X.L. Mao, R.E. Russo, Observation of plasma shielding by measuring transmitted and reflected laser pulse temporal profiles, *Appl. Phys. A*, 1997, **64,** 1–6.

45 B. Xu, Q. Wang, X. Zhang, S. Zhao, Y. Xia, L. Mei, X. Wang, G. Wang, Impulse Transfer to the Surface of Aluminum and Copper from a Pulsed Nd:YAG Laser, *Appl. Phys. B*, 1993, **57**, 277-280.

46 C.T. Walters, R.H. Barnes, R.E. Beverly III, Initiation of laser supported detonation (LSD) waves, *J. Appl. Phys.*, 1978, **49**, 2937-2949.

47 N. Arnold, J. Gruber, J. Heitz, Spherical expansion of the vapor plume into ambient gas: an analytical model, *Appl. Phys. A*, 1999, **69**, S87–S93.

48 Q.L. Ma, V. Motto-Ros, W.Q. Lei, M. Boueri, X.S. Bai, L.J. Zheng, H.P. Zeng, J. Yu, Temporal and spatial dynamics of laser-induced aluminum plasma in argon background at atmospheric pressure: Interplay with the ambient gas, *Spectrochim. Acta Part B*, 2010, **65**, 896–907.

49 J.A. Aguilera, J. Bengoechea, C. Aragon, Spatial characterization of laser induced plasmas obtained in air and argon with different laser focusing distances, *Spectrochim. Acta Part B*, 2004, **59**, 461–469.

50 J.F.Y. Gravel, D. Boudreau, Study by focused shadowgraphy of the effect of laser irradiance on laser-induced plasma formation and ablation rate in various gases, *Spectrochim. Acta Part B*, 2009, **64**, 56-66.

51 D. Bleiner, A. Bogaerts, Multiplicity and contiguity of ablation mechanisms in laser-assisted analytical micro-sampling, *Spectrochim. Acta Part B*, 2006, **61**, 421–432.

52 W. Sdorra, J. Brust, K. Niemax, Basic investigations for laser microanalysis: IV. The dependence on the laser wavelength in laser ablation, *Mikrochim. Acta*, 1992,**108**, 1-10.

53 C. Geertsen, A. Briand, F. Chartier, J.-L. Lacour, P. Mauchien, S. Sjostrom, Comparison between infrared and ultraviolet laser ablation at atmospheric pressure-Implications for Solid Sampling Inductively Coupled Plasma Spectrometry, *J. Anal. At. Spectrom.*, 1994, **9**, 17-22.

54 G. Cristoforetti, Orthogonal double-pulse versus single-pulse laser ablation at different air pressures: comparison of the mass removal mechanisms, *Spectrochim. Acta Part B*, 2009, **64**, 26-34 and Corrigendum, *Spectrochim. Acta Part B*, 2009, **64**, 928-928.

55 C.V. Bindhu, S.S. Harilal, M.S. Tillack, F. Najmabadi, A.C. Gaeris, Laser propagation and energy absorption by an argon spark, *J. Appl. Phys*., 2003, **94**, 7402-7407.

56 D. Bleiner, Z.Y. Chen, D. Autrique, A. Bogaerts, Role of laser-induced melting and vaporization of metals during ICP-MS and LIBS analysis, investigated with computer simulations and experiments, *J. Anal. At. Spectrom.*, 2006, **21**, 910-921.

57 G. Cristoforetti, S. Legnaioli, V. Palleschi, A. Salvetti, E. Tognoni, Effect of target composition on the emission enhancement observed in double-pulse laser-induced breakdown spectroscopy, *Spectrochim. Acta Part B*, 2008, **63**, 312-323.

58 J.A. Aguilera, C. Aragón, V. Madurga, J. Manrique, Study of matrix effects in laser induced breakdown spectroscopy on metallic samples using plasma characterization by emission spectroscopy, *Spectrochim. Acta Part B*, 2009, **64**, 993-998.

59 S.S. Harilal, C.V. Bindhu, M.S. Tillack, F. Najmabadi, A.C. Gaeris, Internal structure and expansion dynamics of laser ablation plumes into ambient gases, *J. Appl. Phys.*, 2003, **93**, 2380-2388.

60 M. Capitelli, A. Casavola, G. Colonna, A. De Giacomo, Laser-induced plasma expansion: theoretical and experimental aspects, *Spectrochim. Acta Part B*, 2004, **59**, 271-289.

61 S.S. Harilal, G.V. Miloshevsky, P.K. Diwakar, N.L. LaHaye, A. Hassanein, Experimental and computational study of complex shockwave dynamics in laser ablation plumes in argon atmosphere, *Phys. Plasmas*, 2012, **19**, 083504.

62 L.I. Sedov, *Similitude et Dimensions en Mecanique*, MIR, Moscow, 1977.

63 Y.B. Zel'dovic, Y.P. Raizer, *Physics of Shock Waves and High-Temperature Hydrodynamic Phenomena*, Academic Press, New York, 1966.

64 A. Bogaerts, Z.Y. Chen, D. Autrique, Double pulse laser ablation and laser induced breakdown spectroscopy: A modeling investigation, *Spectrochim. Acta Part B*, 2008, **63**, 746–754.

65 M. Corsi, G. Cristoforetti, M. Hidalgo, D. Iriarte, S. Legnaioli, V. Palleschi, A. Salvetti, E. Tognoni, Temporal and Spatial Evolution of a Laser-Induced Plasma from a Steel Target, *Appl. Spectrosc.*, 2003, **57**, 715-721.

66 G. Cristoforetti, S. Legnaioli, L. Pardini, V. Palleschi, A. Salvetti, E. Tognoni, Spectroscopic and shadowgraphic analysis of laser induced plasmas in the orthogonal double pulse pre-ablation configuration, *Spectrochim. Acta Part B*, 2006, **61**, 340-350.

67 M. Corsi, G. Cristoforetti, M. Giuffrida, M. Hidalgo, S. Legnaioli, V. Palleschi, A. Salvetti, E. Tognoni, C. Vallebona, Authors' reply to Wen et al.'s comment, *Spectrochim. Acta Part B*, 2005, **60**, 872-875.

68 V.V. Podlubnyi, A.S. Fonarev, Reflection of a spherical blast wave from a planar surface, *Fluid Dyn.*, 1974, **9,** 921–926.

69 Z. Jiang, K. Takayama, K.P.B. Moosad, O. Onodera, M. Sun, Numerical and experimental study of a micro-blast wave generated by pulsed-laser beam focusing, *Shock Waves*, 1998, **8**, 337–349.

70 M. De Rosa, F. Famà, V. Palleschi, D.P. Singh, M. Vaselli, Derivation of the critical angle for Mach reflection for strong shock waves, *Phys. Rev. A*, 1992, **45**, 6130–6132.

71 S. Palanco, L.M. Cabalin, D. Romero, J.J. Laserna, Infrared laser ablation and atomic emission spectrometry of stainless steel at high temperatures, *J. Anal. At. Spectrom.*, 1999, **14**, 1883–1887.

72 S.H. Tavassoli, M. Khalaji, Laser ablation of preheated copper samples**,** *J. Appl. Phys.*, 2008, **103**, 083118.

73 S.H. Tavassoli, A.Gragossian, Effect of sample temperature on laser-induced breakdown spectroscopy, *Opt. Laser Technol.*, 2009, **41**, 481-485.

74 R. Sanginés, H. Sobral, E. Alvarez-Zauco, The effect of sample temperature on the emission line intensification mechanisms in orthogonal double-pulse Laser Induced Breakdown Spectroscopy, *Spectrochim. Acta Part B*, 2012, **68**, 40-45.

75 S. Eschlböck-Fuchs, M.J. Haslinger, A. Hinterreiter, P. Kolmhofer, N. Huber, R. Rössler, J. Heitz, J.D. Pedarnig, Influence of sample temperature on the expansion dynamics and the optical emission of laser-induced plasma, *Spectrochim. Acta Part B*, 2013, **87**, 36-42.

76 J. Register, J. Scaffidi, S.M. Angel, Direct measurements of sample heating by a laser-induced air plasma in pre-ablation spark dual-pulse laser-induced breakdown spectroscopy (LIBS), *Appl. Spectrosc.*, 2012, **66**, 869-874.

77 J.-I. Yun, R. Klenze, J.-I. Kim, Laser-induced breakdown spectroscopy for the on-line multielement analysis of highly radioactive glass melt. Part I: Characterization and Evaluation of the Method, *Appl. Spectrosc.*, 2002, **56**, 437-448.

78 R. Sanginés, H. Sobral, E. Alvarez-Zauco, Emission enhancement in laser-produced plasmas on preheated targets, *Appl. Phys. B*, 2012, **108**, 867-873.

79 G. Cristoforetti, S. Legnaioli, V. Palleschi, A. Salvetti, E. Tognoni, Influence of ambient gas pressure on laser-induced breakdown spectroscopy technique in the parallel double-pulse configuration, *Spectrochim. Acta Part B*, 2004, **59**, 1907-1917.

80 N. Krstulovic, S. Milosevic, Drilling enhancement by nanosecond–nanosecond collinear dual-pulse laser ablation of titanium in vacuum, *Appl. Surf. Sci.*, 2010, **256**, 4142-4148.

81 F. Brygo, A. Semerok, R. Oltra, J.-M. Weulersse, S. Fomichev, Laser heating and ablation at high repetition rate in thermal confinement regime, *Appl. Surf. Sci.*, 2006, **252**, 8314-8318.

82 S.M. Klimentov, P.A. Pivovarov, V.I. Konov, D. Breitling, F. Dausinger, Laser microprocessing in a gas environment at a high repetition rate of ablative pulses, *Quantum Electron.*, 2004, **34,** 537-540.

83 R. Sattmann, V. Sturm, R. Noll, Laser-induced breakdown spectroscopy of steel samples using multiple Q-switch Nd:YAG laser pulses, *J. Appl. Phys. D*, 1995, **28**, 2181-2187.

84 C. Gautier, P. Fichet, D. Menut, J.-L. Lacour, D. L'Hermite, J. Dubessy, Main parameters influencing the double-pulse laser-induced breakdown spectroscopy in the collinear beam geometry, *Spectrochim. Acta Part B*, 2005, **60,** 792-804.

85 T. Čtvrtníčková, L.M. Cabalín, J. Laserna, V. Kanický, Comparison of double-pulse and single-pulse laser-induced breakdown spectroscopy techniques in the analysis of powdered samples of silicate raw materials for the brick-and-tile industry, *Spectrochim. Acta Part B*, 2008, **63,** 42-50.

86 V. Hohreiter, D.W. Hahn, Dual-pulse laser induced breakdown spectroscopy: Time-resolved transmission and spectral measurements, *Spectrochim. Acta Part B*, 2005, **60,** 968-974.

87 M.A. Ismail, G. Cristoforetti, S. Legnaioli, L. Pardini, V. Palleschi, A. Salvetti, E. Tognoni, M. A. Harith, Comparison of detection limits, for two metallic matrices, of laser-induced breakdown spectroscopy in the single and double-pulse configurations, *Anal. Bioanal. Chem.*, 2006, **385**, 316–325.

88 G. Galbacs, V. Budavari, Z. Geretovszky, Multi-pulse laser-induced plasma spectroscopy using a single laser source and a compact spectrometer, *J. Anal. At. Spectrom.*, 2005, **20**, 974–980.

89 N. Jedlinszki, G. Galbacs, An evaluation of the analytical performance of collinear multi-pulse laser induced breakdown spectroscopy, *Microchem. J.*, 2011, **97**, 255–263.

90 A.-M. Matiaske, I.B. Gornushkin, U. Panne, Double-pulse laser-induced breakdown spectroscopy for analysis of molten glass, *Anal. Bioanal. Chem.*, 2012, **402**, 2597–2606.

91 M. Corsi, G. Cristoforetti, M. Giuffrida, M. Hidalgo, S. Legnaioli, V. Palleschi, A. Salvetti, E. Tognoni, C. Vallebona, Three-dimensional analysis of laser induced plasmas in single and double pulse configuration, *Spectrochim. Acta Part B*, 2004, **59,** 723-735.

92 C. Gautier, P. Fichet, D. Menut, J.-L. Lacour, D. L'Hermite, J. Dubessy, Study of the double-pulse setup with an orthogonal beam geometry for laser-induced breakdown spectroscopy, *Spectrochim. Acta Part B*, 2004, **59,** 975-986.

93 F. Bredice, F.O. Borges, H. Sobral, M. Villagran-Muniz, H.O. Di Rocco, G. Cristoforetti, S. Legnaioli, V. Palleschi, L. Pardini, A. Salvetti, E. Tognoni, Evaluation of self-absorption of manganese emission lines in Laser Induced Breakdown Spectroscopy measurements, *Spectrochim. Acta Part B*, 2006, **61,** 1294-1303.

94 F. Bredice, F.O. Borges, H. Sobral, M. Villagran-Muniz, H.O. Di Rocco, G. Cristoforetti, S. Legnaioli, V. Palleschi, A. Salvetti, E. Tognoni, Measurement of Stark broadening of Mn I and Mn II spectral lines in plasmas used for Laser-Induced Breakdown Spectroscopy, *Spectrochim. Acta Part B*, 2007, **62,** 1237-1245.

95 L. Nagli, M. Gaft, I. Gornushkin, Comparison of single and double-pulse excitation during the earliest stage of laser induced plasma, *Anal. Bioanal. Chem.*, 2006, **400**, 3207–3216.

96 R. Sanginés, H. Sobral, Time resolved study of the emission enhancement mechanisms in orthogonal double-pulse laser-induced breakdown spectroscopy, *Spectrochim. Acta Part B*, 2013, **88,** 150-155.

97 G. Cristoforetti, S. Legnaioli, V. Palleschi, A. Salvetti, E. Tognoni, Characterization of a collinear double pulse laser-induced plasma at several ambient gas pressures by spectrally- and time-resolved imaging, *Appl. Phys. B*, 2005, **80**, 559–568.

98 V. Burakov, N. Tarasenko, M. Nedelko, S. Isakov, Time-resolved spectroscopy and imaging diagnostics of single pulse and collinear double pulse laser induced plasma from a glass sample, *Spectrochim. Acta Part B*, 2008, **63,** 19-26.

99 D.N. Stratis, K.L. Eland, S.M. Angel, Enhancement of Aluminum, Titanium, and Iron in Glass Using Pre-ablation Spark Dual-Pulse LIBS, *Appl. Spectrosc.*, 2000, **54**, 1719-1726.

100 D.N. Stratis, K.L. Eland, S.M. Angel, Effect of pulse delay time on a pre-ablation dual-pulse LIBS plasma, *Appl. Spectrosc.*, 2001, **55**, 1297-1303.

101 C. Gautier, P. Fichet, D. Menut,J.L. Lacour, D. L'Hermite, J. Dubessy, Quantification of the intensity enhancements for the double-pulse laser-induced breakdown spectroscopy in the orthogonal beam geometry, *Spectrochim. Acta Part B*, 2005, **60**, 265-276.

102 V. Hohreiter, J.E. Carranza, D.W. Hahn, Temporal analysis of laser-induced plasma properties as related to laser-induced breakdown spectroscopy, *Spectrochim. Acta, Part B*, 2004, **59**, 327– 333.

103 H. Lindner, J. Koch, K. Niemax, Production of ultrafine particles by nanosecond laser sampling using orthogonal prepulse laser breakdown, *Anal. Chem.*, 2005, **77**, 7528-7533.

104 H. Lindner, K.H. Loper, D.W. Hahn, K. Niemax, The influence of laser-particle interaction in laser induced breakdown spectroscopy and laser ablation inductively coupled plasma spectrometry, *Spectrochim. Acta Part B*, 2011, **66**, 179–185.

105 P. Yaroshchyk, R.J.S. Morrison, D. Body, B.L. Chadwick, Quantitative determination of wear metals in engine oils using LIBS: The use of paper substrates and a comparison between single- and double-pulse LIBS, *Spectrochim. Acta Part B*, 2005, **60**, 1482 – 1485.

106 A. Pal, R.D. Waterbury, E.L. Dottery, D.K. Killinger, Enhanced temperature and emission from a standoff 266 nm laser initiated LIBS plasma using a simultaneous 10.6 μm CO_2 laser pulse, *Opt. Exp.*, 2009, **17**, 8856-8870.

107 G. Cristoforetti, S. Legnaioli, V. Palleschi, E. Tognoni, P.A. Benedetti, Crater drilling enhancement obtained in parallel non-collinear double-pulse laser ablation, *Appl. Phys. A*, 2010, **98**, 219–225.

108 R.H. Scott, A. Strasheim, Laser induced plasmas for analytical spectroscopy, *Spectrochim. Acta Part B*, 1970, **25**, 311-332.

109 W.E. Maher, R.B. Hall, Experimental study of effects from two laser pulses, *J. Appl. Phys.*, 1976, **47**, 2486-2493.

110 L. St-Onge, M. Sabsabi, P. Cielo, Analysis of solids using laser-induced plasma spectroscopy in double-pulse mode, *Spectrochim. Acta Part B*, 1998, **53**, 407-415.

111 L. St-Onge, V. Detalle, M. Sabsabi, Enhanced laser-induced breakdown spectroscopy using the combination of fourth-harmonic and fundamental Nd:YAG laser pulses, *Spectrochim. Acta Part B*, 2002, **57**, 121-135.

112 P.A. Benedetti, G. Cristoforetti, S. Legnaioli, V. Palleschi, L. Pardini, A. Salvetti, E. Tognoni, Effect of laser pulse energies in laser induced breakdown spectroscopy in double-pulse configuration, *Spectrochim. Acta Part B*, 2005, **60**, 1392-1401.

113 M.L. Petukh, V.A. Rozantsev, A.D. Shirokanov, A.A. Yankovskii, The spectral intensity of the plasma of single and double laser pulses, *J. Appl. Spectrosc.*, 2000, **67**, 1097-1101.

114 F. Colao, S. Pershin, V. Lazic, R. Fantoni, Investigation of the mechanisms involved in formation and decay of laser-produced plasmas, *Appl. Surf. Sci.*, 2002, **197-198**, 207-212.

115 M. Weidman, S. Palanco, M. Baudelet, M.C. Richardson, Thermodynamic and spectroscopic properties of Nd:YAG–CO2 Double-Pulse Laser-Induced Iron Plasmas, *Spectrochim. Acta Part B*, 2009, **64**, 961-967.

116 C. Gautier, P. Fichet, D. Menut, J. Dubessy, Applications of the double-pulse laser-induced breakdown spectroscopy (LIBS) in the collinear beam geometry to the elemental analysis of different materials, *Spectrochim. Acta Part B*, 2006, **61**, 210-219.

117 M. Oba, Y. Maruyama, K. Akaoka, M. Miyabe, I. Wakaida, Double-pulse LIBS of gadolinium oxide ablated by femto- and nano-second laser pulses, *Appl Phys A*, 2010, **101**, 545–549.

118 X. Mao, A.A. Bol'shakov, D.L. Perry, O. Sorkhabi, R.E. Russo, Laser Ablation Molecular Isotopic Spectrometry: Parameter influence on boron isotope measurements, *Spectrochim. Acta Part B*, 2011, **66**, 604-609.

119 L.B. Guo, B.Y. Zhang, X.N. He, C.M. Li, Y.S. Zhou, T. Wu, J.B. Park, X.Y. Zeng, Y.F. Lu, Optimally enhanced optical emission in laser-induced breakdown spectroscopy by combining spatial confinement and dual-pulse irradiation, *Opt. Exp.*, 2012, **20** 1436-1443.

120 I. Choi, X. Mao, J.J. Gonzalez, R.E. Russo, Plasma property effects on spectral line broadening in double-pulse laser-induced breakdown spectroscopy, *Appl. Phys. A*, 2013, **110**, 785–792.

121 S.Y. Chan, N.H. Cheung, Analysis of Solids by Laser Ablation and Resonance-Enhanced Laser-Induced Plasma Spectroscopy, *Anal. Chem*., 2000, **72**, 2087-2092.

122 W.L. Yip, N.H. Cheung, Analysis of aluminum alloys by resonance-enhanced laser-induced breakdown spectroscopy: How the beam profile of the ablation laser and the energy of the dye laser affect analytical performance, *Spectrochim. Acta Part B*, 2009, **64**, 315-322.

123 S.L. Lui, N.H. Cheung, Resonance-enhanced laser-induced plasma spectroscopy for sensitive elemental analysis: Elucidation of enhancement mechanisms, *Appl. Phys. Lett.*, 2002, **81**, 5114-5116.

124 C. Goueguel, S. Laville, F. Vidal, M. Sabsabi, M. Chaker, Investigation of resonance-enhanced laser-induced breakdown spectroscopy for analysis of aluminium alloys, *J. Anal. At. Spectrom.*, 2010, **25**, 635–644.

Table caption

Table I – Main characteristics, experimental requirements and advantages of the different DP configurations described in this review. The advantages observed in orthogonal pre-spark and collinear configurations have been grouped because of their substantial equivalence.

Configuration	Characteristics	Experimental requirements	Advantages
Orthogonal pre-spark	The ablating pulse is the second one, and the first is needed to create favourable conditions for ablation.	• first pulse irradiance sufficient to ignite a plasma in a gas; • distance between parallel beam and target surface of the order of the plasma size; • inter-pulse delay long enough to allow the first pulse plasma reaching the target surface (longer than approx 100 ns).	• larger ablated mass; • larger atomized mass; • higher plasma temperature; • larger emitting volume; • longer emission persistence. o more homogeneous plasma? o plasma closer to LTE?
Collinear	The effective ablating pulse is the second one, and the first is needed to create favourable conditions for ablation.	• first pulse irradiance sufficient to ignite a plasma; • inter-pulse delay properly chosen so that the density of the first plasma is much lower than the atmospheric one.	
Orthogonal re-heating	The first pulse is the ablating one, the second pulse is used to re-heat the plasma.	• infrared re-heating pulses are absorbed more in typical LIBS plasmas; • short values of the inter-pulse delay give stronger absorption of the second pulse.	• larger atomized mass; • higher plasma temperature; • larger emitting volume.

Figures captions

Figure 1. Atomized ablated mass vs. laser fluence for an aluminium sample in air. In the legend SP stands for single-pulse and DP for double-pulse (orthogonal pre-spark, Δt = 1 μs); the numbers indicate the ambient pressure values in torr. Other details can be found in ref. [54]. Reprinted from Spectrochimica Acta Part B, Vol 64, Pages 26–34, G. Cristoforetti, Orthogonal Double-pulse versus Single-pulse laser ablation at different air pressures: A comparison of the mass removal mechanisms, Copyright 2009, with permission from Elsevier.

Figure 2. Shadowgraphic image of the evolution of the plume and shock wave induced by focusing a single laser pulse in air, and their interaction with the target surface placed at a distance d = 2.4 mm from the focal spot. Interval between frames: 500 ns. Reprinted from Spectrochimica Acta Part B, Vol 61, Pages 340-350, G. Cristoforetti, S. Legnaioli, L. Pardini, V. Palleschi, A. Salvetti, E. Tognoni, Spectroscopic and shadowgraphic analysis of laser induced plasmas in the orthogonal double pulse pre-ablation configuration, Copyright 2006, with permission from Elsevier.

Figure 3. Expansion of the shock wave (solid squares) and plume (empty squares), estimated from data in Fig. 2. The dashed curve is the best fit of shock wave position with a power function $R = at^b$. The dotted line represents a guideline for the eye showing the expansion of the plume. Reprinted from Spectrochimica Acta Part B, Vol 61, Pages 340-350, G. Cristoforetti, S. Legnaioli, L. Pardini, V. Palleschi, A. Salvetti, E. Tognoni, Spectroscopic and shadowgraphic analysis of laser induced plasmas in the orthogonal double pulse pre-ablation configuration, Copyright 2006, with permission from Elsevier.

Figure 4 – Qualitative sketch of the pressure, temperature and particles number density profiles as a function of the radius, according to the Sedov model predictions for the early phase of shock wave expansion.

Figure 5 – Most common geometrical arrangements of the double pulse irradiation: A) orthogonal beams, pre-spark configuration; B) collinear beams; C) crossed beams; D) orthogonal beams, re-heating configuration. Labels 1 and 2 indicate the chronological order of the beams; labels *i* and *ii* indicate the plasma produced by pulse 1 and 2, respectively; d is the distance between the parallel beam and the target surface (the gray bar). Solid lines are used for ablative pulses, dashed lines for non ablative pulses.

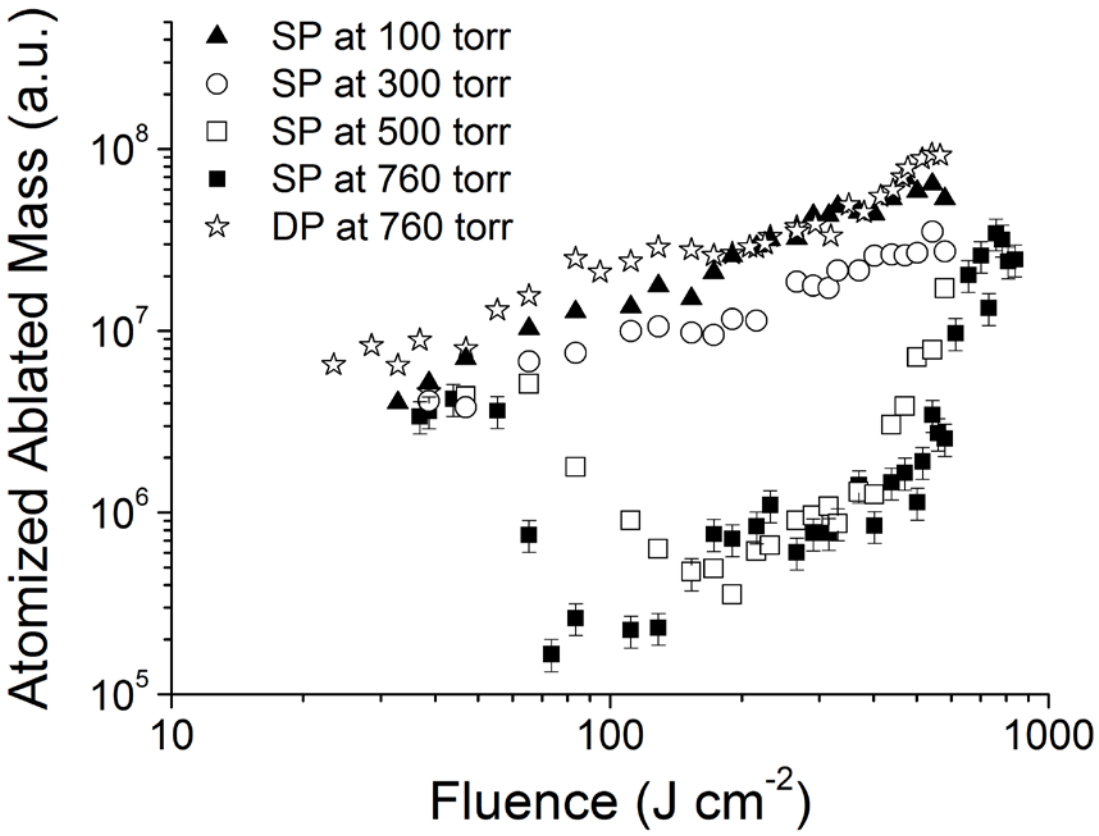

Figure 1

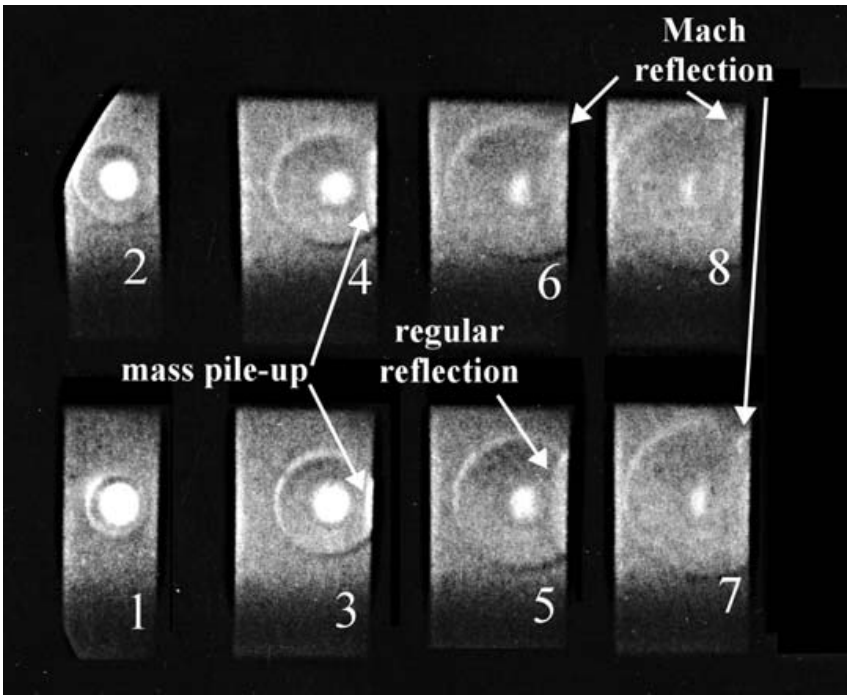

Figure 2

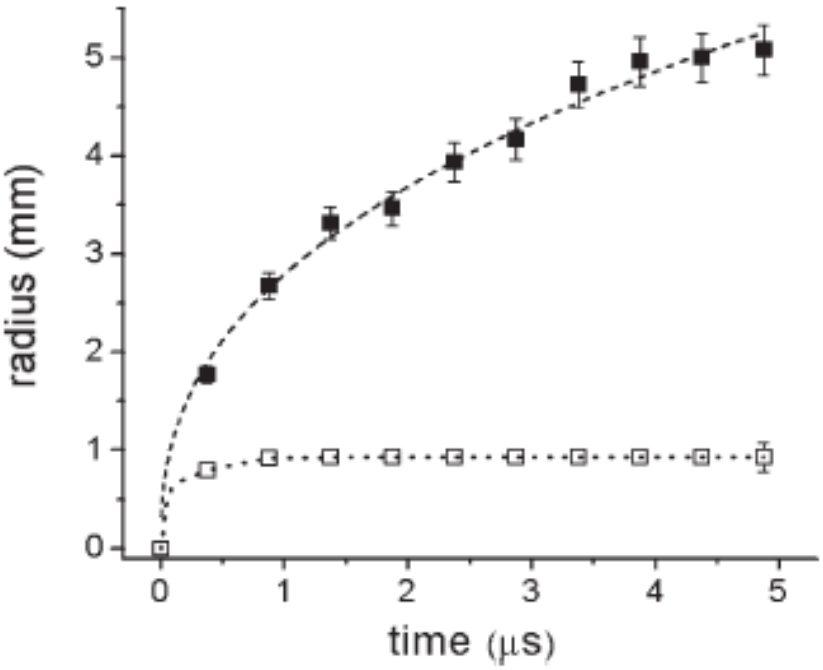

Figure 3

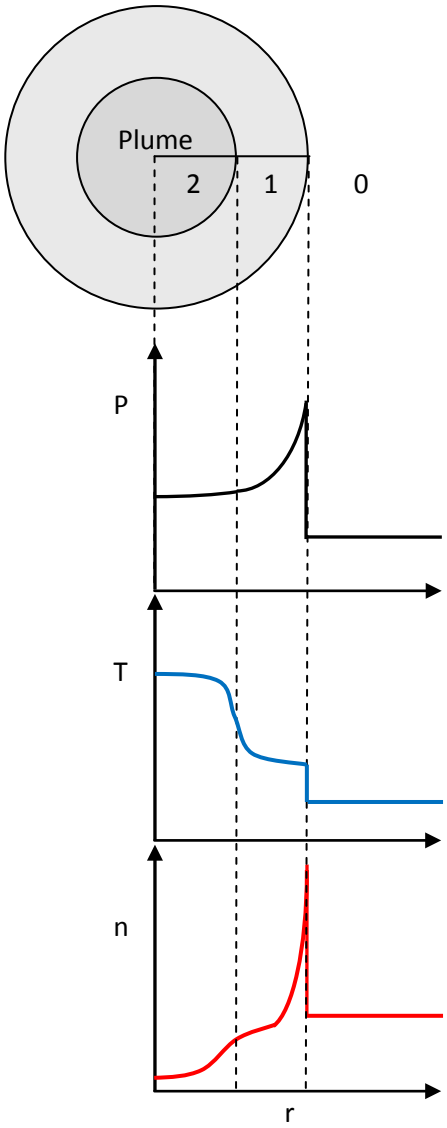

Figure 4

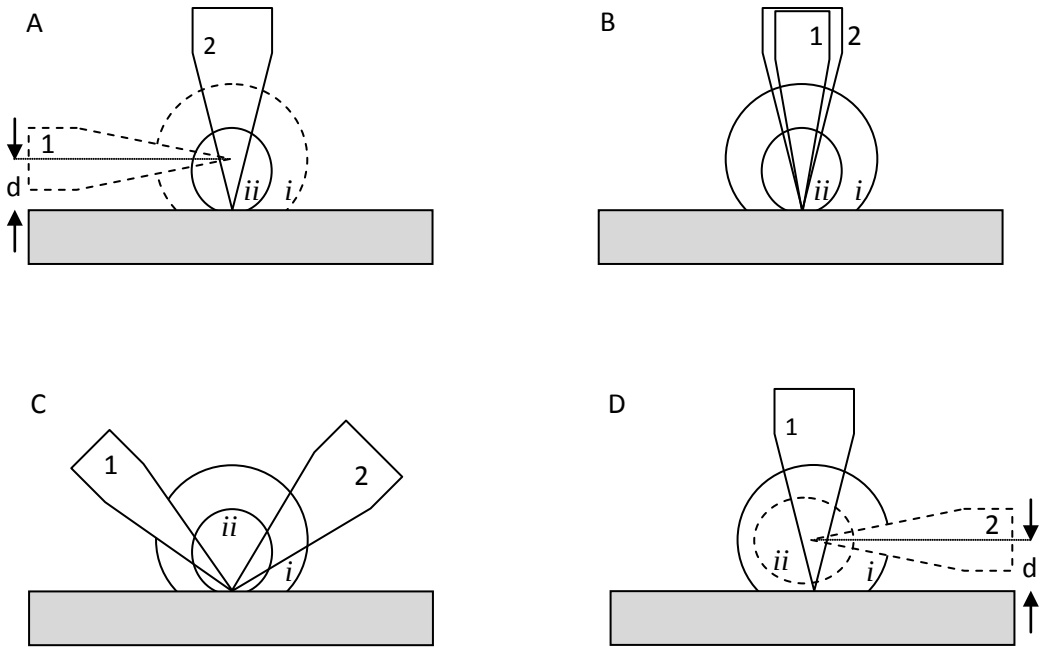

Figure 5